Renewable and Sustainable Energy Reviews 15 (2011) 3717–3732

Contents lists available at ScienceDirect

Renewable and Sustainable Energy Reviews

journal homepage: www.elsevier.com/locate/rser

Review of materials and manufacturing options for large area flexible dye solar cells

Ghufran Hashmi*, Kati Miettunen, Timo Peltola, Janne Halme, Imran Asghar, Kerttu Aitola, Minna Toivola, Peter Lund

New Energy Technologies Group, Department of Applied Physics, Aalto University, P.O. Box 15100, FI-00076 Aalto, Finland

ARTICLE INFO

Article history:
Received 13 December 2010
Accepted 24 June 2011
Available online 6 August 2011

Keywords:
Dye solar cell
Flexible substrates
Roll to roll
Screen printing
Electrolyte

ABSTRACT

This review covers the current state of the art related to up-scaling and commercialization of dye solar cells (DSC). The cost analysis of the different components and manufacturing of DSC gives an estimate on the overall production costs. Moreover, it provides an insight in which areas improvement is needed in order to reach significant cost reductions. As a result of the cost analysis, transferring the technology to flexible substrates and employment of simple roll-to-roll production methods were found the key issues. The focus of this work was set accordingly. In this work, appropriate materials along with their unique fabrication processes and different design methods are investigated highlighting their advantages and limitations. The basic goal is to identify the best materials and preparation techniques suitable for an ideal roll-to-roll process of flexible dye solar module fabrication as well as the areas where further development is still needed.

Contents

1. Introduction 3718
2. Structure of DSC and working principle 3718
3. Cost analysis of DSC 3719
4. Substrates 3719
5. Flexible photoelectrodes 3720
   5.1. Photoelectrode on metal substrate 3720
   5.2. Photoelectrode on plastic substrates 3721
6. Flexible counter electrodes (CE) 3721
   6.1. Platinum catalyst on plastic CE 3721
   6.2. Platinum catalyst on metal CE 3722
   6.3. Carbon based CE 3723
   6.4. Alternative CE catalyst materials 3723
7. Dye sensitization methods 3723
8. Electrolytes 3724
   8.1. Organic liquid electrolytes 3724
   8.2. Ionic liquid electrolytes 3725
   8.3. Quasi solid state electrolytes 3725
   8.4. Solid state electrolytes 3725
      8.4.1. Inorganic HTMs 3725
      8.4.2. Organic HTMs 3725
      8.4.3. Solid state electrolytes with redox couple 3725
9. Sealants and encapsulation 3725
10. Module configurations 3726
   10.1. Parallel grid modules 3726

* Corresponding author. Tel.: +358 505952671.
E-mail addresses: shashmi@cc.hut.fi, sghufranh28@gmail.com (G. Hashmi).

1364-0321/$ – see front matter © 2011 Elsevier Ltd. All rights reserved.
doi:10.1016/j.rser.2011.06.004

10.2. W-type series connection 3726
10.3. Z-type series connection 3727
10.4. Monolithic cell 3727
11. Module production 3727
12. Concluding remarks 3728
Acknowledgements 3728
References 3728

1. Introduction

Photovoltaic (PV) is a promising future source of sustainable electricity production. By 2009, close to 30 GW of PV had been installed producing nearly 25 TWh of electricity [1]. By 2050, 15–30% of all electricity could originate from solar energy according to recent scenarios [2]. At present, most of the PV systems are fabricated with mono or multi crystalline silicon (c-Si) having a market share of 90% [3]. One of the main drawback associated with Si based PV systems is their high cost which limits implementation at large scale. Cutback in production cost by developing more cost effective materials and easy manufacturing of solar cells has become an immediate need in order to make them an affordable way of generating renewable energy.

Dye-sensitized solar cells, also called simply dye solar cell (DSC), are among emerging solar technologies that have potential for low cost along with relatively high efficiency [4]. Moreover, the in practice roll-to-roll mass production concepts from existing industries could be employed for DSC due to its compatibility with preparation on flexible substrates as well as low temperature and atmospheric pressure based manufacturing processes. This is an advantage against the thin film solar cells such as CIGS or a-Si requiring very high investment costs for vacuum equipments [5]. Currently, as much as 40% lower manufacturing line cost per MW for DSC compared with Si solar cells has been claimed [6].

For industrial mainstream manufacturing, DSC offers cheap (Table 1) and endlessly abundant materials such as TiO_2 particles in comparison with solar grade Si obtained from silicon dioxide (SiO_2) by an expensive process [7]. Moreover, unlike for conventional PV technologies, there are basically several different materials to choose from for every DSC component. In addition, several of the materials that can be used for DSCs such as carbon nanotubes [8] have other applications as well which is a clear benefit since there is larger field of scientist working on improving the materials and their preparation methods.

Table 1
Approximated costs of different materials of DSC. The costs presented for substrates are based upon single substrate cost.

Component	~Cost ($/m^2)	Reference
Single substrate		
(1) TCO Glass	12.5-25	[15]
(2) ITO-PET	8–72[a]	[15,12]
(3) Ti (mesh)	15–20	[17]
(4) Ti (foil)	90	[18]
(5) Stainless steel	4	[16]
(6) Al (foil)	0.055	[19]
Other active materials		
TiO_2 particles	0.04	[15]
TiO_2 paste	29	[14]
Internal electrical connections	2.9	[15]
(Dye, electrolyte, CE catalyst)	10.3	[15]
Inactive materials		
(e.g., sealants, encapsulants, additional wiring for external connections and laminating material)	29	[14,15]

[a] The lowest cost was evaluated for PET and ITO separately [15] while the highest price is based on current market value of ITO-PET [12].

Companies such as Dyesol, Sony, and G24i have established pilot production lines testing different configurations, prototypes and modules. The flexible camouflaged solar panel for military [9], solar lantern [10] and backpacks loaded with flexible dye solar modules [11] have been demonstrated as initial consumer applications. In the future, the applications of DSCs could include for instance their integration to roofing and other building materials.

The main objective of this review is to investigate about the appropriate materials and different design approaches which could be used to scale-up the laboratory sized test cells to solar modules. The review begins with the analysis of different costs related to materials and preparation methods which gives the motivation to focus this work on enabling roll-to-roll mass production. Hence, significant emphasis is given to the preparation of flexible electrodes. All the other cell components such as electrolytes are discussed from the viewpoint of manufacturing and hence having emphasis on the processing of the materials. The different DSC module types are also presented and finally the knowledge is gathered as a vision for the production of DSC modules.

2. Structure of DSC and working principle

The basic components of a DSC are the photoelectrode (PE), the counter electrode (CE) and electrolyte as illustrated in Fig. 1. The PE consists of a nanocrystalline TiO_2 layer deposited on substrate with a conducting layer, conventionally a transparent conducting oxide (TCO) coated glass or alternatively flexible substrate such as TCO plastic or metal foil. The TiO_2 layer is sensitized with dye forming a monolayer that absorbs the light. Upon the excitation of a dye molecule by absorbing a photon from sunlight which results in an electron injection into the conduction band of the semiconductor (TiO_2). The external circuit in Fig. 1 depicts this electron and transfers it towards the CE.

The counter electrode is composed of a catalyst layer, typically Pt or C, deposited on another conducting substrate. The gap of PE and CE is filled with an electrolyte solution which contains a redox (I^-/I_3^-) couple that transports the charge back from the CE to PE: the excited dye molecule reduces back to its original state when receives electron from iodide ion presents in the electrolyte solu-

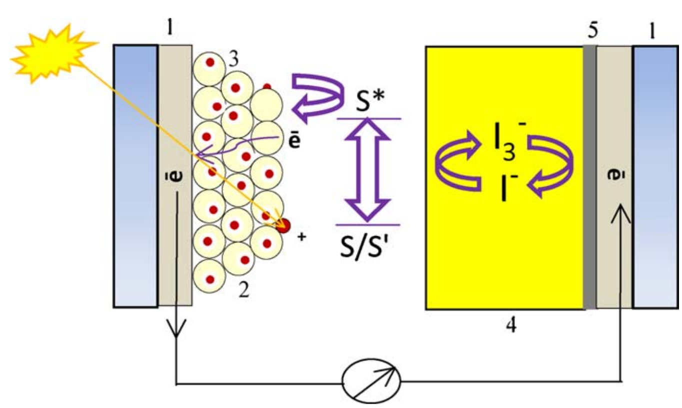


Fig. 1. Structure of the dye solar cell: (1) conducting substrates, (2) TiO_2, (3) dye monolayer, (4) electrolyte, and (5) catalyst layer.

tion. This oxidized iodide ion transforms into tri-iodide ion and reduces back to iodide ion by receiving electron at CE.

3. Cost analysis of DSC

In the cost analysis of an early stage technology such as DSC, it is critical to keep in mind learning curve [12] i.e. with higher production the cost will go down. The main issue is not how high the current costs are but rather how quickly they come down. Recently, Nobuo Tanabe from Fujikura Ltd Japan presented that the current material cost is as high as $93/W_p$ but with 100 MW annual production, it could be lowered down to $0.4/W_p$ [13]. The current high material costs for DSC are understood by the fact that some of the materials are prepared in small quantities mainly for scientific purposes. Similar large cost reductions have been projected also for organic PV (OPV): Indeed, the costs of OPV have been evaluated to decrease much quicker compared to traditional silicon based PV [12]. We expect to see similar effect also for DSCs. Here we investigate reports on the cost for mass production (4–10 MW_p/year) [14,15]. All costs are evaluated in US Dollars ($) with a conversion rate of 1€= 1.3$.

Scaling up from DSC to a module requires better and lower cost materials. These materials can be classified into active and inactive materials [15,16]: the active materials for DSC include TiO_2, dye, electrolyte, CE catalyst, conducting substrates, and electrical interconnects whereas, e.g., the sealants, encapsulants, additional wiring for external connections and laminating material can be identified as the inactive materials as shown in Table 1. In the previous work [15], the substrates have been listed as an inactive material; however, in this discussion we categorize the substrates as active materials due to their essential part in internal electrical connections and their effect on the photovoltaic performance.

The TCO glass substrates has been identified as the most expensive (total for two substrates \$25–50/m^2, Table 1) [15] element of traditional DSCs representing major share (~80%) in the overall active materials cost [15]. Significant (~35%, Table 1) cut down in the cost of active material is expected if the substrate is replaced with flexible plastic (ITO-PET and ITO-PEN). Metal foils can be used to replace one of the electrode substrates and when using stainless steel foil, the costs for one substrate would on average be more than 50% lower compared to ITO-PET and 80% compared to FTO-glass (Table 1). Radical reductions (over 99%, Table 1) in a single substrate cost compared to TCO-glass could be achieved when transferring the technology to very low cost metals such as aluminum. These kinds of large costs reductions give an additional motivation for the use of flexible substrates in addition to suitability for roll-to-roll production. There are however stability issues related to the lower cost metals which have been discussed in Sections 5.1 and 6.2.

As low cost as \$0.04/m^2 has been evaluated for TiO_2 particles [15], however, in another study the costs of the ready-for-use TiO_2 paste has been estimated almost 1000-times higher, ~\$29/m^2 [14]. This reveals that in addition to the raw material costs, attention needs to be given also to the easy and low cost manufacturing of the pastes and inks. Following costs have been evaluated for other active components: \$2.9/m^2 for electrical connections and \$10.30/m^2 for rest of the materials such as (dye, electrolyte and catalyst layer) (Table 1) [15].

A significant proportion of the total cost (17% of conventional glass based DSC) is allocated also to the inactive materials ~\$29/m^2 [14]. Reduction of those costs is therefore also highly motivated. Zweibel estimated \$5/m^2 each for strut-bolt and metallic frame encapsulation for thin film PV modules [16]. The application of flexible DSC modules is likely to be different (e.g., mobile applications) and would therefore not require such a robust and expensive mounting. Hence, this cost can be omitted from the total cost of inactive materials. Other components such as flexible laminating material and sealants are not very expensive (~\$3/m^2 each) [15]. However, it is unclear whether the laminating materials described in Ref. [15] are sufficient to prevent, e.g., water intrusions. Actually such efficient blocking layers may increase costs significantly.

Moreover, the cost of equipments and tools for module manufacturing is favorable to DSC due to the advantage of non-vacuum processes [5]. Despite of many processing steps are needed for DSC, the projected price for a 10 MW/year manufacturing facility for batch processing of glass based DSCs is in between \$7.25/m^2 and \$11.60/m^2 [15] which is already clearly lower compared to thin film solar cells \$32/m^2 [20]. By implementation of roll-to-roll mass production techniques and low temperature processing, the manufacturing costs are expected to decrease even further. For instance for organic solar cells (OSC), which is another new generation PV technology, the cost estimations for equipment vary much more (\$3.3–59.60/m^2) [15].

There are also other factors affecting the overall production costs such as module warranty, service charges for maintenance of production equipment and salaries for labor and staff which can be recognized as overhead cost [15,20]. In the past, this overhead cost for thin film PV has been estimated to \$34/m^2 [20]. However for DSC, this cost is expected to be much smaller due to low maintenance cost for non-vacuum equipment. Kalowekamo and Baker estimated a minimum cost of \$14.50/m^2 for DSC overheads in comparison to a cost of \$13.78/m^2 for OSC [15]. No estimation for maintenance charges of production equipment was included.

Based upon above mentioned factors, the production cost for glass based DSCs with current techniques and materials has been estimated to a total costs in between \$150 and 220/m^2 [14,15]. With module efficiency of ~5–8% this results in estimated ~\$3–4/W_p price [14,15] in comparison with ~\$3/W_p of silicon based PV modules [15]. The costs of glass based DCSs are expected to decrease to ~\$1.4/W_p in near future as the DSC technology matures for high volume production [14]. By manufacturing DSCs on light weight flexible substrates and implementation of roll-to-roll processing large cost reductions are gained from the overall material costs, manufacturing and even overhead cost. According to the data presented above, we project that the overall costs of flexible DSCs could even be halved compared to glass based batch processes DSC technology leading to a total cost less than \$1/W_p.

4. Substrates

As mentioned in the previous section, the selection of suitable substrates is the key factor affecting the cost but in addition it determines appropriate preparation methods of a DSC and hence also affects the performance and stability. The essential requirements for an ideal substrate are high conductivity, transparency in visible spectral region, non-permeability combined with high stability and low cost [21–23].

Traditional engineering of DSC utilizes glass sheets coated with fluorine doped tin oxide (FTO). Despite of their good stability against oxygen and water permeability, it has been appraised that these glass sheets consume high cost among all active material of the cell as mentioned in the previous section [14,15]. Furthermore due to the fragility, rigidity, heavy weight and shape limitations, these glass sheets cannot be used for roll-to-roll (R2R) production. Based upon these facts, the focus of the research has been shifted towards alternative, low cost, light weight and mass reproducible flexible substrates.

The flexible metal sheets for instance stainless steel (StS), titanium (Ti) and nickel (Ni) has been employed as alternative substrates for DSC [23–29]. Their key features including flexibility, low

cost, e.g., StS [21], very low sheet resistance (R_{Sheet}) compare to TCO films on glass [23], non-permeability and suitability to high temperature treatments. The metal substrates can be employed in a PE [29–31] or CE [24,26] configurations. As metals are non transparent, the other electrode serves as a window electrode, e.g., plastic sheet with a transparent oxide layer coating.

The key question in the case of metals is stability [24]. In this regard the properties of several metal sheets (StS, Ni, Cu, Al) have also been investigated before employing them in DSC [24–26]. The chemical stability tests revealed that only StS sheets were stable whereas, e.g., Cu and Al sheets dissolved in electrolyte [24,26]. Though StS have passed the soaking tests [24–26], they still have stability problems when used in complete DSC [24,32,33]. Good stability results have been achieved with Ti foils [34] but they have much higher cost (\$90/m^2 Table 1) [18]. By changing to alternative electrolytes that are less prone to cause corrosion, a wider range of metals, in particular lower cost metal such as Al (\$0.055/m^2, Table 1) [19], could be feasible options. A viable alternative electrolyte that works with Al and could result in sufficient stability has recently been reported [35]. Further investigation is, however, needed.

The main advantages offered by conducting plastics, e.g., indium doped tin oxide polyethyleneterephtalate (ITO-PET) and indium doped tin oxide polyethylenenaphtalate (ITO-PEN) are flexibility and light weight make them compatible for the R2R production [36,37]. Sufficient transparency (80% at 550 nm) [22] and sheet resistance (R_{Sheet}) of ~10 Ω/Sq as well as good chemical stability in electrolyte is also achieved by employing these sheets in DSC in comparison with metals [24,38]. Nonetheless, these plastic sheets restrict the manufacturing temperature below 150 °C [37,39]. Also the permeability of plastics arouses stability questions as water and other contaminants may diffuse into DSC [22]. Plastics are also brittle in nature due to UV irradiation [40] which rouses significant stability concerns [41]. The degradation by UV can, however, be avoided by using a suitable protective coating [12]. Another important factor that affects the use of ITO coated plastics is the scarcity of ITO which will limit the production in very large scale and even at this point makes ITO expensive [42]. Hence alternative TCO coatings on plastics are being sought for.

Carbon nanotubes (CNT) have been extensively experimented as a replacement to TCO in numerous electronic and optoelectronic devices [43,44]. The CNT exhibit good electrical conductivity, large surface area and robust flexibility along with chemical inertness and can be mass producible [45,46]. However, the difficulty is to get both high transparency and low R_{Sheet} at the same time [47,48]. At the moment the best compromise is R_{Sheet} of 60–95 Ω/sq with high optical transparency (>80%) on flexible substrate [49]. In other words, the characteristics do not yet match those of the best TCO layers but with improved engineering of CNT films this may be achieved. However, in addition to reach good enough electrical performance, the high cost (\$64/m^2) [50] of CNT films may also become a question.

Light weight, highly conductive and flexible metal wire meshes have also been employed in DSC to achieve a semi transparent conductive layer without the use of TCO [17,51–53]. The titanium metal meshes have low R_{Sheet} (1×10^{-3} Ω/sq.) and are able to cope with the high temperature of TiO_2 sintering process [52]. Compared to back side illuminated metal based DSC, the DSC with a metal mesh based photoelectrode have lower optical losses [51,54]. Recent implementation of these meshes yield an overall efficiency in between 3% and 5% [17,52].

These cells are, however, comparatively thick due to the thickness of metal wires [17,52] which may limit the efficiency in particular in the case of high viscosity electrolytes such as ionic liquid electrolytes. Other factors such as space between knitted titanium wires can also increase the resistance between wires and has been a key question to overall performance of the cell [52]. Moreover, the Ti mesh does not result in cost reductions compared to TCO coated glass (Table 1).

A better solution could be to use chemically stable printed metal grids patterned in 10 μm scale [55] by using, e.g., Ti ink. Fabrication of such ink has not yet been demonstrated. Alternative strategy, as in the case of metal sheets, is to use a non-corrosive electrolyte such as solid state polymer electrolytes with commercially available Ag ink printed grids. Such printed metal grids can have 70–80% of open area and still result in lower than 1 Ω/sq sheet resistance which is one order of magnitude lower compared to commonly used TCO layers [56]. With lower sheet resistance the cell efficiency could be improved and/or the size of a unit cell in a DSC module enlarged leading to improved aperture ratio and higher efficiency in a module level.

5. Flexible photoelectrodes

It is possible to adapt modern printed electronics technology for fabrication of DSC by using light weight and flexible sheets. For the production of flexible photoelectrodes (PE), a continuous coating process for deposition of TiO_2 layer is required. Several different methods have been presented in particularly for the low temperature preparation of PEs while trying to reach as high efficiency as with high temperature sintering used in the case of TCO-glass substrates. High efficiency (>7%) PEs have been fabricated on both flexible plastic and metal substrates [57–59].

5.1. Photoelectrode on metal substrate

Metal based PE have an edge over plastics due to their compatibility with high temperature sintering process to get high quality and highly adhesive TiO_2 film with good inter-particle connections between them as well as non-permeability. However, the DSC with metal based PE requires illumination from CE (back side) [27,57,59]. The optical losses such as absorption of light by the catalyst and the electrolyte layer result in a decrease in the current production and hence also in the overall cell performance [27,57]. Nevertheless the cell configuration can be optimized by controlling the thickness and the composition of the catalyst layer and electrolyte to achieve good results: loss in the cell efficiency 24% due to reverse illumination [57].

The highest efficiency of flexible DSC (8.6%) is with metal based PE [57]. In this cell the TiO_2 was deposited on a StS coated with ITO and SiO_x layers [57]. The metal based PEs such as the ones on StS have shown sufficient characteristics for R2R production for instance, crack-free and highly adhesive films on StS were reported after the bending and standard tape tests [30].

However in the case of StS, the stability is a critical problem as the cell can lose even 80–90% of performance in couple of hours of 1 sun illumination [34,38]. The stability of the StS PE cells with the additional layers such as used in Ref. [57] has not been reported.

So far only the PE deposited on Inconel and Ti among the metal based PEs have been shown to pass 1000 h light soaking test in 1 sun [34]. The highest reported efficiency on flexible DSC equipped with Ti based PE is 7.2% with *FF*, short-circuit current density (J_{SC}) and open circuit voltage (V_{OC}) of 0.68, 13.6 mA cm^{-2} and 0.78 V, respectively [59]. The additional benefit of the Ti based PE is very low recombination current from the substrate to the electrolyte [34], which is expected to improve the cell performance significantly in low light conditions. Moreover, there were no additional resistances between the substrate and the TiO_2 layer in the case of Ti contrary to the case of Inconel [34]. The drawback associated with Ti sheets is its higher cost (~\$41) compared to other metals that have been considered as PE substrates (e.g., Al, StS) [60].

Nevertheless, the compensation may be achieved by combining Ti coating on an inexpensive metal substrate.

Currently, work is going on to develop non-corrosive electrolytes to be used with low cost metals such as Al [35], which would widen the selection of suitable metals also as photoelectrodes. Another future development could be to change from high temperature processing of PE to low temperature methods which would be a significant advantage from the manufacturing point of view but challenge in regard of performance. We believe that this kind of progress is possible since there has been such a huge development of the efficiency of plastic based PEs (∼76% in 10 years) [61] leading to 8.1% current record efficiency of plastic DSCs [58]. Naturally the methods developed for plastics could be adapted also to metals. However, the main benefit of metals as photoelectrode substrates, i.e. suitability to high temperature production, would then be irrelevant. Then it would be more beneficial to use plastic photoelectrode substrate in order to minimize optical losses and deposit the counter electrode on metal. The low temperature methods and metal based counter electrode are discussed in more detail in the later sections.

5.2. Photoelectrode on plastic substrates

As mentioned before the critical challenge for plastic PE technology lies in the low temperature preparation of TiO_2 layer since the maximum temperature these plastics can endure is around 150 °C. Normally the TiO_2 layer is sintered in high temperature (400–500 °C) to get good electrical contact between the particles. Additionally, the typical titania paste contains organic binder and viscous solvents which remove in the high temperature sintering process. As a result numerous techniques (Table 2) have been developed to fabricate low temperature plastic PE electrodes [62–65].

One of the very early methods of low temperature preparation was the hydrothermal synthesis of metal oxide nanocrystals [64,66,67] in which a paste is obtained by mixing TiO_2 crystals with the Ti-monomers (e.g., $TiOSO_4$ or $TiCl_4$) [64]. Autoclaving of deposited paste layer originates a reaction which transforms Ti-monomers into TiO_2 [64,66,67]. This transformed TiO_2 constructs crystalline necks between the original TiO_2 particles and makes firm connections [64,66]. This low temperature (LT) method gave very good efficiency of 6.4% on fluorine doped tin oxide (FTO) glass [64]. However, paste with these precursors cannot be applied on ITO-PET film since it damages the ITO layer [66,67]. Alternative Ti-monomer for instance Ti (IV)-tetraisopropoxide (TTIP) has been replaced with the aforesaid precursors [67]. Well adhesive films were produced with adequate mechanical stability [66]. However, the cells deposited on ITO-PET with this method exhibit a low efficiency of only 2.5% [66].

Another similar technique is called chemical vapor deposition (CVD) of Ti-alkoxide [68,69]. Conversion of a gaseous precursor for instance $Ti(OC_3H_7)_4$ or $[(CH_3)_2CHO]_4Ti$ into TiO_2 takes place if introduced in the vicinity of existing TiO_2 particles layer. Participation of microwave [69] or UV-treatment [68,69] in CVD promotes crystallization and necking of TiO_2 that encase the existing TiO_2 nanoparticles [68,69]. Mechanically stable, adhesive films with uniform morphology were gained [68]. PE fabricated with this technique illustrated already significantly higher (3.8% efficiency [68]) compared to the hydrothermal method [66].

The UV treatments have been investigated further and promising results (an overall efficiency up to 5.2%) have been reached in the case of glass substrates by employing UV laser beam technique [70]. For ITO-plastic, the typical process includes a laser synchronized with pulse laser deposition [71,72] or with spray deposition [73]. The TiO_2 suspensions have been deposited by means of an aerosol with a carrier gas (nitrogen) [73]. Simultaneous rapid heating with a laser beam fabricates a porous, uniform and crack less film [73]. Nevertheless the agglomerates of nanoparticles are also claimed to occur due to fast evaporation of the solvent [73]. The DSCs based on plastic foil prepared using this method yielded an efficiency of 3.3% [73].

Duerr et al. introduced a so called 'lift off' method in which a sintered high quality TiO_2 layer is prepared on another substrate and then transferred onto plastics [65]. Firstly, a screen printed TiO_2 layer is primarily applied to a thin gold layer on a glass substrate [65]. Secondly after sintering at 450 °C, the TiO_2 layer is removed from the glass by dissolving the gold layer with an electrolyte (I^-/I_3^-) solution [65]. Finally, the TiO_2 layer is transported and pressed on ITO-PET (already coated with an adhesive thin titania film) via high stress. The method proposes a unique combination of high-temperature sintering along with the compression method, which can be implemented for R2R production. An overall conversion efficiency of 5.8% was achieved with this method [65].

The binder free titania paste have also been made in order to avoid post treatments of the layers. The idea has been demonstrated by obtaining low energy conversion efficiency of 1.9% [74]. Later on, Miyasaka et al. reached an efficiency of 5.8% with highly viscous and binder free paste that was coated on ITO-PEN substrate (Table 2) [75,76]. One of the keys to this result was using surface tension reducing agent *t*-butanol in the TiO_2 paste [75]. In the optimization of layer thickness, 12.5 μm was found to be the best [76]. The resulting films were highly adhesive which is essential to R2R production. This method is ideal for high volume R2R production and eliminates the additional process steps and costs.

Another interesting procedure is the mechanical compression [61] which offers R2R production compatibility of nanoparticle films on plastic substrates. The method involves static or continuous pressing [61,65,77,78] of TiO_2 suspensions deposited on substrate. The idea of the pressing is to form firm contacts between neighboring nanoparticles. Static press based DSC exhibits somewhat higher mechanical strength and over all light to electricity conversion efficiency (3–4%) in comparison to continuous pressing (2–3%) [61].

Recently, Yamaguchi et al. announced 8.1% efficiency for plastic PEs using pressing as a one procedure (Table 2) [58]. The good efficiency was attributed to the removal of impurities by a UV-O_3 treatment [58]. They noticed that after the threshold pressure 50 MPa the efficiency was the highest and the optimal layer thickness was 6–7 μm [58]. Comparing this 8.1% efficiency with the 11.1% reported by Chiba et al. on glass [4], it illustrates that DSC technology can be shifted from rigid glass substrates to flexible plastic substrate with satisfactory conversion efficiency.

6. Flexible counter electrodes (CE)

The key parameters for an efficient counter electrode (CE) are low charge transfer resistance (R_{CT}) for the tri-iodide ion reduction, chemical stability in the electrolyte solution and mechanical stability [79,80]. The optical properties also have some effect such as reflectance from the CE. If the cell is reversely illuminated such as when using metal as photoelectrode, the optics plays a critical role as the CE needs to be semitransparent [54]. The CE can be fabricated with different materials and techniques.

6.1. Platinum catalyst on plastic CE

The platinum (Pt) loaded substrates exhibit low R_{CT} and efficient kinetic performance for the tri-iodide reduction [81,82]. Pt catalyst layer can be deposited on the flexible substrates by different low temperature methods for instance sputtering [82,83], chemical [30,84] and electrochemical [24,59,85,86] deposition. Regarding the stability of Pt counter electrode is generally regarded to be good,

Table 2
Different methods for the preparation of flexible photo-electrodes (PE) and reported cell performance at 1 sun illumination (100 mW cm^{-2}).

Substrates	Pre-treatment	Paste	Deposition	Post-treatment	η (%)	Reference
StS		TiO_2, α-terpinol and ethyl cellulose	Doctor blading	Sintering 600 °C	8.6	[57]
ITO-PEN	UV–O_3	TiO_2–water paste	Doctor blading	Mechanical pressing	8.1	[58]
Ti		TiO paste	Screen printing	Sintering 325–500 °C	7.2	[59]
ITO-PEN		(1) TiO_2 F-5 Showa titanium t-butanol and water (1:2), (2) aqueous collide TiO_2 (brookite) 21 wt.%, 25% HCL with pH4 and 75% ethanol, (3) mixture of (1) and (2)	Doctor blading or screen printing	Heating 110–125 °C	5.8	[76]
Glass		Stock solution of Ti^{4+} Titanium(iv) isopropoxide, triethanolamine and DI water	Thermal hydrolysis	Mechanical compression	5.8	[65]
ITO-PET		TiO_2 F-5 Showa titanium tert-butyl alcohol and acetonitrile (95:5) mixture	Electrophoretic deposition	CVD/UV 254 nm	3.8	[68][a]
ITO-PET		TiO_2 P25 Degussa, water, nitric acid, Triton, ethanol and methanol	Spray deposition or pulsed laser deposition	UV 248 nm pulse width 20 ns	3.3	[73]
ITO-PET		TiO_2 P25 Degussa [Ti(IV)-tetraisopropoxide]	Hydrothermal crystallization	Autoclaving 100 °C 12 h	2.5	[67]
ITO-PET		TiO_2 P25 Degussa, 20 wt.% ethanol	Doctor blading	Mechanical pressing	2.3	[77]

[a] This efficiency was measured at 85 mW cm^{-2}.

e.g., long DSC lifetimes have been reached with thermally platinized catalyst layer [24,25]. There are, however, some concerns about the stability of Pt in elevated temperatures (80 °C) [87] and additionally the mechanical stability, i.e. adhesion of Pt to the substrate, varies with different deposition methods [54].

The chemical and electrochemical methods propose Pt reduction from its salt solution and they can be customized for R2R production. The chemical reduction comprises by an additional reducing agent [84] where as electric field has been applied for electrochemical reduction [85]. These methods have compared on transparent conductive oxide (TCO) glass substrate [81,82] showing that the chemically deposited Pt was more stable and exhibited high exchange current for redox couple compared to the electrochemically deposited Pt [81]. In our previous tests, we have also noted the weak adhesion of Pt catalyst layer to the ITO-PET when using the electrochemical method [54]. In addition, in our tests, the quality of the chemically deposited film varied much: there were evenly distributed films as well as films with inhomogeneous clusters [54]. Both chemical and electrochemical deposition can be used to produce semi transparent CEs and their use has resulted in the highest efficiencies of 8.6% [57] and 7.2% [59], respectively, in cells with metal based PEs.

Sputtering, on the other hand, is typically well reproducible and high quality resulting also good mechanical stability Pt films on glass [82]. Pt sputtered glass CE attributes very low R_{CT} (0.05 Ω-cm^2) [82] and very high efficiency (11.18%) [88]. Roll to roll sputtering of different layers has been demonstrated for organic PV [89] which could also be adapted for Pt films of DSC. Platinum sputtered plastic films have been used by Yamaguchi et al. for 8.1% efficiency cell [58].

Another way is to spray thermally attached Pt enrich inert powder suspensions (Sb:SnO_2) by adding it in a volatile solvent for example ethanol [61,77,80]. The purpose was to increase the surface area and to minimize R_{CT}. However, with the increase of active area, the amount of Pt in the catalyst film also increases and so does the related cost. Further pressing of the film promotes mechanical integrity and adhesion [77,80]. This R2R compatible method claimed 2.3% efficiency of the cell [77].

In the view of the low cost roll-to-roll production, the best option would be to use simple printing technique for the deposition of the catalyst layer. Related to this, Chen et al. demonstrated recently Pt deposition on ITO-PEN by screen printing resulting in overall efficiency 5.41% [90]. The optimal screen printing Pt paste was developed by dissolving 0.6% $H_2PtCl_6 \cdot H_2O$. in terpineol which lead to R_{CT} of 0.53 Ω-cm^2 [90]. Non uniform film with Pt clustered nano particles was obtained [90]. The quality of the film was then further improved by introducing hydrothermal treatment [90]. The main downside of this treatment is that the overall process, in particular the hydrothermal treatment, is very time consuming (several hours) and needs further development to be suited to fast roll-to-roll production.

6.2. Platinum catalyst on metal CE

As discussed earlier, metals have certain benefits over plastic substrates such as non-permeability, much lower sheet resistance and lower cost (Table 1). Metal counter electrode could therefore be a good option to be used with plastic photoelectrode. Similar to PE, several metal based CEs have been demonstrated [24–27,91].

Pt catalyst layers have been deposited on StS sheets by using sputtering, thermal and electrochemical deposition methods [24,25]. Relatively poor performance with thermal and electrochemical deposition is reported [24]. Furthermore, the DSCs fabricated with StS based CE prepared with thermal deposition corroded [32]. The best efficiency (5.24%) with DSC with StS CE has been achieved with Pt sputtered catalyst layer [24]. Our recent investigation revealed that the ~10 nm sputtered Pt layer was effective also in preventing corrosion [92]. Other protecting coatings for instance SiO_x layer have also been suggested [57].

Ti exhibits good chemical stability in the electrolyte and can be used even without protective coatings [92–94]. Ti based CE prepared using electrodeposition and thermal deposition methods exhibit low R_{CT} (0.4 Ω-cm^2) in comparison with ITO and FTO substrates [95] which is an important characteristic to obtain fast exchange rates for tri iodide reduction. Also the low R_S (1 mΩ/sq.) of Ti sheets may be used to improve the overall efficiency of large area

DSC [52]. At present, the best conversion efficiency of DSC obtained with Ti based CE is 7.7% [95].

Similar to plastic counter electrodes, development of simple low temperature and low cost printing methods are needed for metal counter electrodes. For some other type of catalysts such as carbon, there are already such methods. Those are discussed further in the next sections.

6.3. Carbon based CE

Due to high catalytic activity, Pt is usually used for CE. Nonetheless, to reach lower cost and improved chemical stability in electrolyte, alternative materials have been investigated [61,80,96]. Some of these catalysts materials, such as porous carbon, can even be deposited with directly roll-to-roll adaptable techniques as mentioned before [97].

Carbon black is an inexpensive material which is mainly used in newspaper inks, printing inks and has also been employed as a black pigment for inkjet or toners [98]. Good electrical conductivity and fast exchange rates for tri-iodide reduction are the key features of carbon black when used as a relatively thick (10–20 μm) porous layer [79,96,99]. When using an even thicker carbon layer (∼60 μm) [79], the sheet resistance (R_{Sheet}) of the catalyst layer becomes as low as 5–10 Ω/Sq [79] resulting in that other conducting layers are not needed at the counter electrode side. This is an important characteristic in particular for monolithic cells. The carbon suspensions that have been used in different CE configurations for instance monolithic cells include typically high surface area carbon nano particles (activated carbon), highly conductive and binding materials such as graphite and TiO_2, respectively [79,100–102]. The carbon layers can be, e.g., screen printed and they are commonly sintered at around 400–500 °C to get attachments between particles (c.f. porous TiO_2 on PE) [97,103]. The carbon powder CE has still challenges concerning layer thickness, cracks and adhesion in particular when applied in the monolithic design [104].

This common preparation method can be applied directly on metal substrates such as StS or graphite sheets [21]. As high efficiency as 9.15% was reached when using carbon loaded StS substrate as CE [21]. As the carbon layer is porous, an additional corrosion protective layer is still needed on StS.

Using flexible graphite sheets with porous carbon catalyst layer is a good way to get sufficient chemical stability in addition to good electrical activity, heat resistivity and low charge transfer resistance (1.2 Ω-cm^2) [105,106]. A good overall efficiency of 6.46% was gained with these pure carbon CE based DSC [96]. Note that the bare graphite sheets do not give sufficient area for the catalyst reaction resulting in low fill factor (*FF*) (0.37) and efficiency (2.88%) of the cells [96] and hence the porous catalyst layer is also needed.

Carbon suspensions have also been deposited on plastic substrate with doctor blading [61,77] and spraying [80] followed by in both cases pressing to improve the contacts between the particles (c.f. preparation of low temperature TiO_2 layers [61,80]. The sprayed electrodes gave the good R_{CT} results (0.5–2 Ω-cm^2) [80]. However in particular, the very thick films had poor flexibility. In our recent study, we were able to improve the flexibility of the carbon catalyst layer by introducing a novel gel based carbon paste [101]. The photovoltaic performance of these cells was good (Table 3) and CEs could be rolled even to 3 mm bend radius without any visible cracking [101]. The long term stability of these electrodes needs still to be determined [61,77,101].

The good conductivity and high specific surface area in a carbon nanotube (CNT) motivates their study as counter electrode material. The use of carbon nanotube based CE is likely to make conductive and transparent films and the additional conductive layer (FTO/ITO) can be omitted from the cell [8]. The studies have mostly been made using FTO glass as a substrate. The adhesion of a single wall carbon nanotubes (SWCNT) film on FTO was found durable by performing a scratch test [107]. The SWCNT electrode [107] exhibited low R_S (1.8 Ω/sq.) and a good efficiency of 4.5% in comparison with carbon filaments [108] and nanohorn [109] based CE. Despite of FTO glass substrates, the CNTs have also been implemented on metal substrates [110]. Drop casting of SWCNT solution (obtained by ultrasonication of 2 mg SWCNT powder and 10 mg water) was performed on StS CE at 150 °C [110]. DSCs, with these StS CE yielded an overall efficiency of 3.92% and remained stable in a 1000 h light soaking test under AM1.5 at 25 °C [110]. It has recently been suggested that the hybrid of carbon nanotubes and carbon powder could result in a catalyst film with both very good catalytic activity but more importantly lower sheet resistance [111]. Low sheet resistance is needed in particular when no additional conducting layer is used on the counter electrode such as in monolithic cells [8].

6.4. Alternative CE catalyst materials

The conjugated polymers for example polyaniline [112], polypyrrole [113], (PEDOT) doped either with p-toluenesulphonate (TsO) or polystyrenesulphonate (PSS) [114] have also been tested as alternative catalyst material to replace Pt catalyst layers in DSC. Their benefits are structural flexibility, good conductivity, and low cost [54,115].

Among them, the PEDOT films can be distinguished due to uniformity [116], good stability and transparency in visible light region [117,118] along with very low R_{CT} (0.8 Ω-cm^2) [116]. The best efficiency (7.93%) till date with these alternative polymer catalysts is comprised by electro-polymerization of PEDOT layer on TCO glass substrate [116]. In this method the substrate receives a precursor ion through an applied electric field and accomplishes firm contact with it [116]. Both the suitability of the electrochemical process of plastic substrate and the stability of the resulting catalyst film need still to be shown.

Due to the hydrophobic nature of plastics (e.g., ITO-PEN), it is sometimes difficult to get films of high transparency and good adhesion [54,58,115]. A composite (TiO_2.ITO/PEDOT-PSS) polymer paste demonstrated by Muto et al. enables screen printing on ITO-PEN sheets [115]. The adhesion stability was detected to be good in the mechanical scratching and bending tests [115]. The DSC equipped with these semi-transparent TiO_2.ITO/PEDOT–PSS based CE exhibited 4.38% efficiency in comparison to ones with Pt coated FTO glass CE giving 5.41% [115].

In the comparative studies, PEDOT-TsO has given lower R_{CT} compared to PEDOT-PSS [54]. Several methods for instance, spin coating, spraying and casting of PEDOT-TsO have also been tested on TCO glass and plastic substrates [54,119]. Spin coating has given well working, semi transparent PEDOT-TsO films [54,119]. The problem with the spin coating method is, however, that there is significant loss of materials and it is not suited for R2R production. With spraying, a thick, non-transparent layer of PEDOT-TsO is required to reach low R_{CT} whereas the casted layers were very uneven resulting in poor performance [54].

7. Dye sensitization methods

The sensitization or staining of the dye can be performed by different methods [27,120,122]. Traditional method involves direct immersion of TiO_2 coated substrates into dye solution from several hours to overnight in order to obtain good and uniform distribution between dye molecules and TiO_2 layer [27]. This technique has been adopted for large area DSC production by using a sealed staining chamber [122,123]. The concentrated dye solution can be transported to the staining chamber by generating a turbulent flow

Table 3
Different methods for preparation of CE and reported cell performance.

CE substrate	Method	Catalyst	R_{CT} (Ω-cm²)	J_{SC} (mA cm^{-2})	V_{OC} (mV)	*FF*	*η* (%)	Reference
FTO-glass								
FTO-Glass	Sputtering	Pt		17.73	846	0.75	11.18	[88]
FTO-Glass	Doctor Blading	C	0.74	16.8	790	0.685	9.1	[120]
FTO-Glass	Electro polymerization	PEDOT-PSS		15.0	693	0.76	7.93	[116]
Plastics								
ITO-PEN	Chemical deposition	Pt					8.6	[57]
ITO-PEN	Sputtering	Pt		14.5	750	0.75	8.1	[58]
ITO-PEN	E. chem deposition	Pt		13.6	780	0.68	7.2	[59]
ITO-PEN	Screen printing/H. thermal	Pt	0.53	10.1	682	0.78	5.41	[90]
ITO-PEN	D. blading S. printing	PEDOT-PSS					4.38	[115]
ITO-PEN	Doctor blading	C	23	11.2	700	0.54	4.24	[101]
ITO-PEN		SWCNT-EOI		6.81	660	0.36	1.63	[121]
Metals								
Graphite	Doctor blading	C	1.2	13.1	703	0.702	6.46	[96]
StS	Sputtering	Pt		12.4	703	0.60	5.24	[24]
StS	Drop casting	SWCNT		9.21	660	0.64	3.92	[110]
StS	Chemical deposition	Pt	19	15.10	650	0.36	3.6	[26]

through a circulation pump [122,123]. Possible inadequacy associated with this method is the dye absorption at CE while draining it through the outlet port, which might leads to diminished catalytic activity [79]. Additionally, it is a slow process (~2 h) but can be speed up to some extent by heating up the dye solution [123].

Combining PE and CE via high temperature sealing utilizes a so called "first seal then stain" or glass frit sealing method [122,124]. In this method, the PE and CE are first joined together by means of glass soldering at 600 °C to prevent dye decomposition [122]. For staining, the dye solution is driven through the in/out channels [122,124]. Nevertheless, it consumes extra amount of dye solution than simple immersion. Therefore the study about the spatial distribution as a function of key parameters such as pressure and dye concentration is called for. Suitable methods for such spatial distribution study are the segmented cell method [125] and photocurrent imaging [126].

Furthermore, techniques such as pumping normally take hours for dye staining and cannot be integrated in R2R manufacturing. For optimal preparation of DSCs, advanced techniques suitable for fast roll-to-roll production as well as dyes with rapid adsorption are needed for the deposition of dye. The optimum way to deposit dye would be printing and, e.g., Sony company is pursuing such methods [127].

8. Electrolytes

The electrolytes employed in DSC can be categorized into organic liquid, ionic liquid, quasi solid state and solid state electrolytes. The motivation to study other electrolyte compositions besides traditional organic liquids has arisen from the chemical and mechanical stability issues of organic liquid electrolytes which are critical in particular when using alternative flexible substrates. The main advantage of ionic liquid electrolytes over the organic liquids is that ionic liquids have zero vapor pressure i.e. they do not evaporate. The quasi solid electrolytes are typically organic liquid electrolytes which are gelatinized with polymers or particles in order to reach mechanical stability. The solid state electrolytes differ greatly from the above mentioned as they typically comprise only of polymers and thus cannot leak out or evaporate [128,129].

8.1. Organic liquid electrolytes

Traditional DSC is filled with a liquid electrolyte solution which is mainly composed of an organic solvent (such as acetonitrile and 3-methoxypropionitrile), a redox couple (I^-/I_3^-) and additives such as 4-tert butylpyridine (TBP) or N-methylbenzimidazole (NMBI) [4,23]. The best cell efficiency (11.1%) [4] thus far and interestingly enough also the longest cell lifetime (20 000 h in 0.8 sun at 55-60 °C) [130] has been achieved with the DSC equipped with the liquid electrolyte. These good results can be at least partly explained by fact that the organic liquid based DSCs are far more investigated compared to the alternatives and hence it is understandable that there has been also significant development. Nonetheless, their role is critical due to volatility, leakage and corrosion [33]. As the corrosion is caused by iodine, the corrosion problems could perhaps be overcome e.g. with an alternative redox couple [131,35]. The components of electrolytes exhibit chemical and photochemical degradation for instance the bleaching of electrolyte due to reduction of iodine (I_3^-) [132]. Presence of harmful liquid chemicals such as acetonitrile (regulated here in Finland) in consumer products is questionable and is one more significant reason to investigate alternatives.

The electrolyte filling method is important from both production and performance point of view. In small scale a typical method of filling liquid electrolytes is to have drilled holes on the counter electrode and apply the liquid through them. In large area cells, this way of filling is slow and it may leave air bubbles in the cell. Hence, in particular for the filling of large area DSCs [122,124], the electrolyte filling has been performed with the same setup which is described in the last section for staining [122,124]. Depending on module design, inserting the electrolyte after assembly may require the filling and sealing a huge amount of separate compartments, which may be slow and prone to cause defects [122,124].

Ideally all the components of electrolyte should be distributed uniformly throughout the cell. However, our studies with segmented cell have clearly shown performance variations in photovoltaic parameters due to non uniform adsorption of TBP [125]. The V_{OC} was found highest near the electrolyte filling hole decreasing gradually towards the end of the cell [125]. To overcome the performance losses caused by the non-uniformity, it has been suggested that either the electrolyte composition or the deposition method needs to be modified [125]. This calls for the study of other commonly used additives such as N-methylbenzimidazole (NMBI). The use of segmented cell method [125] for this study instead of photocurrent imaging which gives only distribution of J_{SC} [126,133] is recommended as electrolyte typically has significant effect also on all the photovoltaic parameters.

As the current electrolyte filling method is both unsuited for roll-to-roll production and has been shown to cause non-uniformities leading to performance losses [125], it would best to device a novel deposition method. Such as in the case of deposition of dye, application of electrolyte would be best done with printing. Transferring

from this traditional type of liquid electrolyte to alternative electrolytes may also make the printing of the electrolyte easier.

8.2. Ionic liquid electrolytes

In order to prevent possible leakage from DSC, the volatile and liquid solvents have been replaced with ionic liquid electrolytes [134,55]. These ionic liquid electrolytes are chemically and thermally stable [135,136] and some of them have also passed light soaking test at 60 °C and thermal stress test at 80 °C [33].

The main challenge of ionic liquids to getting high performance as the viscosity of the electrolyte is about 100-times higher compared to organic liquids [134,137]. There are, however, additional charge transfer mechanisms (such as Grotthus mechanism) which ease the diffusion of ions to some extent. The high viscosity of the ionic liquid electrolytes also hinders the use of those deposition methods that are employed for applications of liquid electrolytes. On the other hand, the viscous structure offers other possibilities: These electrolytes can be filled with the staining method, e.g. Sastrawan et al. demonstrated the filling of $30 \times 30\,cm^2$ modules [123,124] by reducing the viscosity of ionic liquids at 70 °C [123,124]. Furthermore, it is also possible to insert the ionic liquids before cell sealing, e.g., with screen printing it on to the photoelectrode thus making filling holes and their sealing unnecessary [138]. This technique offers rapid and reproducible R2R production compatibility for flexible substrates. On the other hand, filling the right amount of electrolyte before cell assembly is problematic. When there is not enough electrolyte, the gap will not fill completely and, when there is an excess, electrolyte is pushed between the sealant and the substrates [122]. It has been suggested that a few escape holes could be used for the excess electrolyte to be pushed out of the cell in a controlled way [122].

8.3. Quasi solid state electrolytes

Quasi solid state electrolytes (QSSEs) or gel polymer electrolytes (GPEs), derived by encaging organic liquid electrolyte in polymer chains have been actively integrated in DSC [139–141]. Numerous polymers and nanoparticles such as polyvinylpyridine (PVP) [142], polyacrylonitrile (PANI) [143], polyethyleneoxide (PEO) [144], poly(vinylidene fluorideco-hexafluoropropylene) (PVdF-HFP) [145], TiO_2[145], graphite [145] and silica [146] have been proposed to gelatinize the electrolytes. Among them the electrolyte polymerized with PVdF-HFP shows relatively high ionic conductivities ($3.85 \times 10^{-3}\,S\,cm^{-1}$) even at room temperature [145], good thermal stability [146,147] and high efficiency (7.3%) [147]. The PVdF-HFP has been used also with TiO_2, graphite [145] and silica (SiO_2) nano particles [146] to gelatinize liquid electrolytes. E.g., the initial efficiency (4.69%) recorded at 10 wt.% PVdF-HFP was enhanced up to 6.04% when 0.25 wt.% graphite nano particles were introduced [145]. The PVdF-HFP electrolyte needs to be hot when injected to the cells and in that regard their application is more complex compared to liquid electrolytes. However, when the electrolyte is cooled down, it solidifies and it might be easier to manage compared to liquids.

8.4. Solid state electrolytes

Solid state DSC (SSDSC) utilizes either inorganic hole transport materials (HTMs) for example CuI [128], CuSCN [148], organic HTMs such as (2,2′,7,7′-tetrakis-(N,N-di-p-methoxyphenylamine)-9,9′-pirobifluorene) spiro-OMeTAD [149,150] or solid-state electrolyte containing I^-/I_3^- redox couple [129,151] as medium. It is obvious that solid state electrolytes are interesting due to potential for eliminating the leakage problem. For monolithic designs solid state electrolyte can be directly applied through casting [152] or vacuum filling technique [153–155].

8.4.1. Inorganic HTMs

The inorganic HTMs electrolytes have been prepared by simply mixing CuI (0.6 g) in acetonitrile [156] or by dissolving CuSCN (1 g) in n-propyl sulphide (2 ml) [157]. The solution can be directly applied and dried (∼75–125 °C) on TiO_2 substrate by spraying and hot plate respectively. Despite of easy up-scalable preparation method and good conductivity ($10^{-2}\,S\,cm^{-1}$) [158,159], the quick crystallization growth of CuI has shown to result in incomplete filling of the pores and insufficient contacts with the TiO_2 particles which in turn attributes low cell efficiency (<1% [156]) and instability of the cell [128,160,161]. Crystal growth inhibitors such as 1-methy-3-ethylimidazolium thiocyanate and triethylamine hydrothiocyanate (molten salts) have been successfully used to control the crystallization of CuI crystals [128,160–163]. A slightly increased efficiency (3.0%) was observed in DSC cells equipped with these inhibitors when compared with the efficiency (2.9%) of DSC containing only HTMs [162].

8.4.2. Organic HTMs

Organic HTMs such as Spiro-OMeTAD possess low hole mobility ($2 \times 10^{-4}\,cm^2/VS$) [163,164] in its intrinsic structure, the performance could, however, be enhanced ($1 \times 10^{-3}\,cm^2/VS$) when engineered with lithium salt ($Li(CF_3SO_2)_2N$) [165]. Moreover, the Spiro-OMeTAD exhibit fast recombination rates than liquid electrolytes [166,167]. On the other hand, promising results for the filling of the pores of TiO_2 layer has been achieved due to small size and good wettability which improves the overall photovoltaic performance (∼4%) of the cell [168,169] in comparison to other hole transport materials (∼0.5%) [170].

The typical recipe for Spiro-OMeTAD based electrolyte concerns mixing of Spiro-OMeTAD (0.17 M), tert-butylpyridine (TBP) (0.12 mM), and $LiN(CF_3SO_2)_2N$ (19.5 mM) in chlorobenzene which turned to a solution and can be applied by spin coating [171,172]. More than one volt (1087.5 mV) open circuit has already been achieved with a conversion efficiency of 3.17% when equipped with Spiro-OMeTAD electrolyte [171].

Recently Grätzel and co-workers demonstrated doctor blading of Spiro-OMeTAD based electrolyte solution [149]. This is important in particular for R2R production when compare to spin coating where material loss could be relatively high [149]. Additionally same conversion efficiency (3.01%) with doctor blading was achieved in comparison with spin coating method [149]. Nevertheless the stability of these cells has not been reported.

8.4.3. Solid state electrolytes with redox couple

Nanocomposite gel electrolytes integrated with redox couple (I^-/I_3^-) for SSDSC are suggested as an alternative solution to organic and inorganic HTMs due to their low photovoltaic performance [151,173,174]. The synthesis requires a sol–gel method which uses solidifying agent (tetra-n-butyl titanate) in order to solidify the liquid electrolyte containing ethylene glycol and redox couple (I^-/I_3^-) [174]. High ionic conductivity ($1.4\,mS\,cm^{-1}$) has been gained by increasing amount of NaI (0.008–0.04 M) in the electrolyte [174]. DSC attributed a conversion efficiency of 3.14% with this electrolyte [174]. Further improvement in efficiency (3.597%) was observed with an additional mixing of polypyrrole nanoparticles [174].

9. Sealants and encapsulation

The performance challenges to get DSCs to practical applications are mainly associated with their instabilities during long term operation [33,124]. These instabilities have been attributed, e.g., due to volatility of the solvent present in the electrolyte solution,

its thermal stress and vapor pressure [33,175]. In addition to that the intrusion of water and oxygen, temperature changes and effects caused by UV light harm its basic operation [22,33]. Therefore there is a vital requirement for a good sealing material to tackle the above mentioned challenges.

Glass frit is often used on the edges of the glass based DSC to seal the electrolyte [123,124]. The sealant also acts as a spacer to keep the counter electrode from touching the photoelectrode [123]. Glass frit has certain benefits, in particular, is chemically very stable and it can be deposited by screen printing [124]. It does, however, require high temperature sintering at about 600 °C meaning that it can be used basically only in DSCs deposited on glass i.e. cannot be implemented on fast low temperature roll-to-roll process.

A typical low temperature solution is the use of thermoplastic films such as Surlyn. For plastic modules, Ikegami et al. prepared a flexible seal by applying hot melt (Surlyn) at 120 °C [22]. The initial photovoltaic performance was maintained for 220 h when exposed to high temperature (55 °C) and humidity conditions (95%) [22]. In practice, Surlyn films have low softening temperature and therefore the cells sealed with it can handle temperatures only below 60 °C which is too low for outdoor applications [176]. Bynel hot-melt [146] has been used as a replacement to Surlyn. Ideally the low temperature sealant would also be printable.

Additionally, DSCs are often laminated with a protective coating which acts as a barrier against intrusion of external contaminants [12]. The lamination may be performed by bonding a foil gasket between substrate and protective coating [122] or by applying an adhesive (such as 467MPF from 3 M) [12,177,178] on protective barrier foil (e.g., Ceramis ultra barrier films from Alcen) [179] or Teonex PEN and Melinex polyester films [180] and then laminated over substrate in a R2R fashion [12] The typical lamination temperature for these materials ranges from ~20 to 200 °C [181].

10. Module configurations

Up-scaling small laboratory test cells into large prototypes for industrial manufacturing tackles several issues for instance current collection grid and its protection, sheet resistance of the substrates, electrolyte filling and cell sealing. Numerous cell structure concepts have been developed and illustrated [79,122,124,138]. Mostly the large area DSCs have been fabricated on glass substrates [122,124], but also DSCs based on ITO-PEN sheets have also been demonstrated [22].

10.1. Parallel grid modules

A parallel module is made by depositing several areas of dye-sensitized TiO_2 on a common substrate and using highly conductive metal fingers (typically Ag) on the electrode (Fig. 2a) is a simple way to overcome the high resistance of the TCO layer. Although there are many physically isolated active areas, they are all electrically connected in parallel and behave as one unit cell [124,182]. As most metals corrode in the iodine electrolyte [55], the use of an additional blocking layer between the metal current collector and the electrolyte is required. Such blocking layer can be a polymer hot-melt foil (low temperature), glass frit (high temperature) or ceramic glaze (high temperature) [124,175,183–185].

A wide range of different current collecting patterns has been used to decrease surface resistance [55,124]. The objective is to make a design with minimum amount of electrolyte filling holes, inactive area (i.e. high aperture ratio) and small distance between the electrodes to facilitate tri-iodide diffusion in the electrolyte. The two last mentioned requirements limit the conductivity of the fingers considerably and in practice one finger cannot be much longer than 5 cm and not thicker than few tens of micrometers. One possibility is to make grooves on the electrode substrate [186]: according to our calculations a 1 mm deep groove would increase the height and hence the conductivity of a finger by two orders of magnitude compared to a 10 μm finger. Grooving may also help to make the fingers narrow since the protecting layer only has to go on top of the conductor [186]. Grooving could allow the use of inferior conductors such as titanium in the current collectors and, since Ti does not corrode in the electrolyte, space taking blocking layers could be omitted [186].

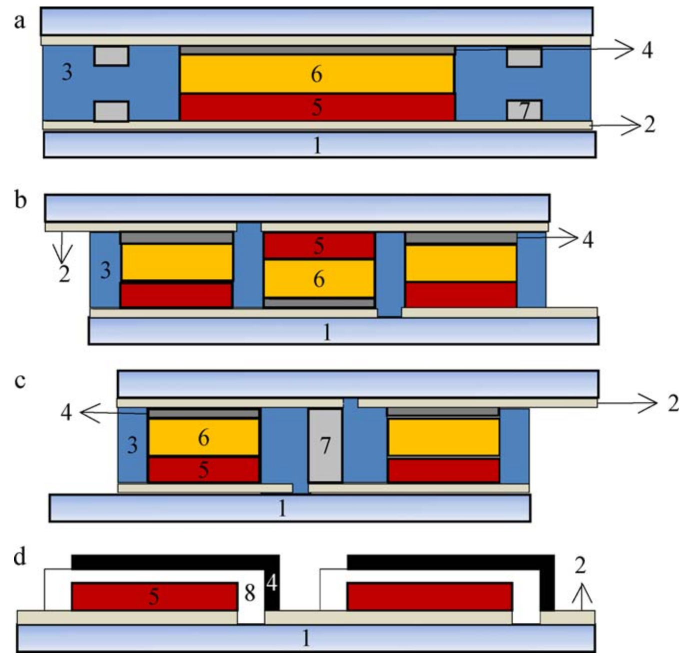


Fig. 2. The schematic cross section of (a) parallel module design, (b) W-type series connection, (c) Z-type series connection and (d) monolithic dye solar cell. The cell components are numbered as follows: (1) substrate, (2) TCO layer, (3) protective layer (sealant), (4) catalyst, (5) dye coated TiO_2, (6) electrolyte, (7) silver grids, and (8) insulating spacer. A Z-type series connection is shown in figure (d), on the right where the carbon layer is in contact with the TCO layer of the next cell.

The fingers are connected to highly conductive bus bars outside the cell for long range current transport [187]. The active area (2246 cm^2) has been demonstrated for parallel type with the conversion efficiency of 5.89% [187]. The stable performance of such DSC panels has been observed during short term stability tests (1 week), however, no long term stability test results have been reported [182].

10.2. W-type series connection

The advantages offered by W-type modules are simple structure by avoiding inter-connections, large active area, simple fabrication procedure and low cost [188–190]. In the W-type module, a series connection created by placing both photo- and counter electrodes on substrates in an alternating pattern, as illustrated in Fig. 2b. By using series connections which decrease current densities, the ohmic losses can be decreased. The conductive surface is scribed appropriately to produce a series connection. Series connected cells are in different electric potentials, which causes the redox couple to separate in the electrolyte. This phenomenon is called electrophoresis and it decreases cell performance. Therefore each cell must be in a closed compartment.

Additionally, since the photo and counter electrodes are fabricated on the same substrates, the deposition and post treatment of the TiO_2 layer, size of the active area and absorption of light by Pt catalyst and electrolytes are the key issues [189–191]. The

fact that both photo and counter electrodes are deposited on the same substrates means that manufacturing methods for each electrode type cannot be separately optimized. The high transparency requirement for the counter electrode rules out several alternative catalyst layers such as porous carbon. There is typically a mismatch in J_{SC} and efficiencies of individual cells due to difference of illuminations for the photo and the counter electrode [188]. Hence, the W-type module generates about 10-20% less power than a standard sandwich design with Z-interconnect module (see Section 10.3) [54,191]. The W-type modules have yielded an overall efficiency up to 8.4% with an aperture area of 26.47 cm^2. Nevertheless, the stability testing of these modules have not been reported [192].

A natural active area pattern for this type of cell is long thin stripes connected in series. TCO surface resistivity restricts stripe width to about 1 cm. The non-active area required by the electrolyte barrier can be 1 mm wide or even less with a suitable printing method. As with all fixed series connections, there is a risk that the current-voltage characteristics of the cells do not match resulting in decreased module performance. It has been suggested that dye solar cells would not require bypass diodes as only about 0.5 V of reverse bias is needed to force current through one cell and this reverse current might not affect cell stability [193,194] however, this needs still further investigation.

10.3. Z-type series connection

A Z-type series connection is a design similar to the W-type in regard of the main idea which is to a form series connection to reduce ohmic losses. The only differences are that the photo and counter electrodes are on separate substrates and the series connection is realized with conductive interconnect material in the case of Z-type connection (Fig. 2c). As in all series connected cells, mass transfer must be prevented using suitable barriers between the individual cells. Because of the barriers and interconnect, the dead area is larger in Z-type cell than in a W-type cell. To reduce the dead area, a non-porous interconnect that is not corroded by electrolyte would be ideal to avoid additional barriers and to simplify the device fabrication.

Due to interconnects, there is larger resistance decreasing *FF* as well as a larger dead area compared to the W-type cell. However, the Z-type is expected to have higher efficiencies because both electrodes can be separately optimized and light does not enter through the counter electrode side for half of the cells [188,191].

A novel design which is known as 'Meander module' has been developed to increase the width of a unit cell in order to have fewer unit cells in a module [124]. The benefit of this design is smaller number of electrolyte filling holes that need to be sealed. In Meander modules current collecting fingers are added to unit cells to increase their width. In practice the unit cells form serpentine type structure. The unit cells are joined together with Z-type series connections. A typical Z-type cell width is less than 1 cm whereas meander cell can be 5 cm wide reducing the number of holes to one fifth [124]. The largest demonstrated meander modules having an active area of 30×30 cm^2 fabricated with this method yielded an overall efficiency of 3.1% [124].

10.4. Monolithic cell

The monolithic cell design differs considerably from typical sandwich configurations both in respect to both materials and cell assembly [79]. The main difference is that the cell is deposited on a single substrate, i.e. the counter electrode on top of the photoelectrode (Fig. 2d) [79,97,100]. After the usual titanium dioxide deposition an insulating porous spacer layer is added in order to keep the photo and counter electrodes from touching each other [100]. This spacer layer is usually obtained by mixing insulator such as zirconium dioxide (ZiO_2) and light reflecting particles such as TiO_2 nanoparticles (rutile structure) [79]. CE catalyst layer is normally a think porous carbon as mentioned in Section 4.3. The porosity of the carbon layer facilitates charge transfer due to high surface area and enables the application of electrolyte without purpose-drilled holes [97,100]. A good sheet resistance is also required from the carbon film as there is no other conducting layer on the counter electrode.

Monolithic cells have lower efficiencies than sandwich cells as the insulating spacer hinder the diffusion of ions [79,195]. A natural way to make a large module is to use the Z-type series connection as shown in Fig. 2d [100,196]. The spacer is simply printed over the titanium dioxide layer and the counter electrode over the spacer so that it makes contact with the TCO of the next unit cell [100]. However, an additional barrier to block electrolyte transfer between adjacent cells is still needed. The monolithic design is also suitable for the parallel connection scheme since there is no height limitation to the current collectors. A monolithic minimodule consisting of four individual cells with an active area of 3.38 cm^2 each has recently been demonstrated by Pettersson et al. [97]. Module efficiencies of 5% at light intensity of 200 W/m^2 were achieved after 2200 h of light soaking at 1000 W/m^2 and 50 °C [97].

11. Module production

The fabrication of DSC modules does not essentially require a clean room environment or vacuum conditions [5,197]. As discussed in the earlier section there are R2R compatible printing methods for the deposition TiO_2, catalyst layers and pastes for current collecting grids. Careful optimization is still required. At present, the most popular technique to coat aforementioned materials is screen printing [59,76,104] which can be induced in a R2R manufacturing process [198]. In fast R2R mass production, it would be best to use only cheap low temperature processes and in that regard there is still room for development. For instance, most of interesting low temperature methods has not been investigated from the stability point of view.

Here we propose a futuristic view for the fabrication of flexible dye solar cell modules (Fig. 3) and at the same time summarize the findings from the previous sections. Due to the low cost and high conductivity, metal should be used as one of the substrates. When using metals without additional expensive coatings (insulator layer + additional conducting layer), only parallel connected modules can be made without cutting the metal. Hence the cells would be stripes which could then be laminated together close to each other to form a module. Window electrode would be on plastic in which conducting layer would not be based on ITO but, e.g., a very fine printed metal grid leading to higher performance, lower cost, and better availability. The lower sheet resistance of printed metal meshes would allow making wider stripes than with traditional TCO layers contributing to higher module efficiency.

When having all low temperature processes, it is best to use plastic as the photoelectrode substrate so that optical losses can be minimized. A viable solution for the PE production could be a binder free TiO_2 paste, which does not require post heating, combined with pressing [75,76].

One of the parts most in need of a development is the application of dye. It normally takes hours for dye staining and is inappropriate to integrate in R2R manufacturing. Ideally, also the dye would be printable and currently such techniques are under investigation by commercial players [127].

The electrolyte composition and filling might actually be the most challenging part. The best case would be to use a screen printable non-corrosive solid state electrolyte layer. E.g., the recently developed new Spiro-OMeTAD based electrolyte solution [149] might fill these requirements. In particular much more stability

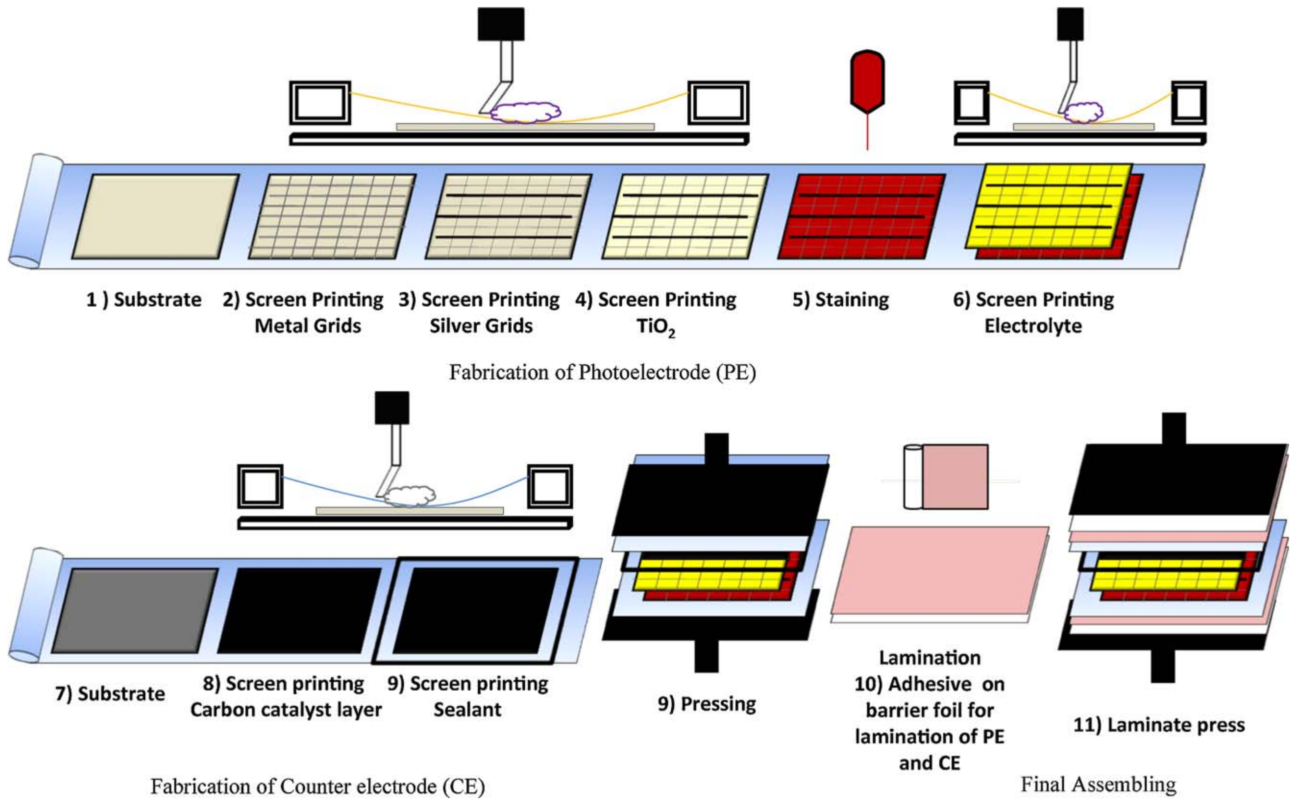


Fig. 3. Process flow diagram for fabrication of a flexible DSC module.

testing is still needed. The non-corrosiveness would be the key to using cheap metal substrates, e.g., Al, readily available Ag inks for preparation of fine metal grid to replace TCO, omitting protective layers for current collectors and hence minimizing the inactive space.

Counter electrode could also be applied by screen printing and there are suitable methods for the preparation of screen printable carbon paste [97,102]. The use of carbon catalyst layers also provide the way to get rid of expensive ITO layer on the substrate if a plastic substrate is also used on the counter electrode.

Cell assembly can be realized by applying adhesive on one of the electrodes and compressing the substrates together. Polymer sealant gel material is preferable due to easy applicability and integration in process line with a screen printing step. This step can be performed by using continuous press method [61]. In last step, the barrier foil to prevent moisture penetration is laminated with adhesive. At the lamination stage the metal based unit cell stripes can be put together in small intervals and before lamination the current collectors can be placed between the cells.

12. Concluding remarks

In the cost analysis section, it was suggested that via roll to roll production even lower than $\$1/W_p$ price may be achieved. This technique can only be adapted with flexible substrates such as metal and plastic sheets. When pushing the cost as low as possible, very cheap metal substrates (e.g., Al) and alternative conducting layers for plastic substrates (e.g., printed extra fine Ag grid) are needed. Moreover, the manufacturing methods should be cheap, easy and fast to reach high volume production. From this point of view it would be best to omit, e.g., high temperature treatments.

In broader spectrum, some low temperature processes and materials have been developed for example screen printing can be used for the deposition of different kinds of layers and there are recipes to produce low temperature titania paste to achieve highly efficient cells (8.1%) [58]. There are, however, many challenges associated with the different components of the cell that need significant attention.

In particular, the questions related to the composition and the deposition of the electrolyte is still very problematic. In the view of low cost production and user-friendliness, a non-corrosive solid state electrolyte that could be for instance deposited by screen printing would be preferable. However, significant improvement of solid state electrolytes is required as the overall conversion efficiency is not currently very impressive, only ~4.05% [168,169]. In addition to the electrolyte, also the dye deposition requires some optimizations. A viable futuristic solution could be a screen printable dye monolayer instead of using conventional filling methods such as pumping of the dye solution.

A common denominator in the field of low temperature materials and methods as well as with non-corrosive and/or solid state electrolytes is the almost complete lack of stability studies. Sufficient cell lifetime is, however, a critical aspect in the view of a commercial product. Hence we want to impress that in addition to improving the photovoltaic performance and manufacturability of the dye solar cells, the stability issues need to be more strongly incorporated to the studies.

Acknowledgements

G.H. is thankful to T. Miyasaka, F.C. Krebs, A.R. Andersen, M. Ikegami and S. Ahmad for the information they have provided. This work was funded by the Academy of Finland.

References

[1] Global market outlook for photovoltaics until 2014. EPIA publications. http://www.epia.org/fileadmin/EPIA_docs/public/Global_Market_Outlook_for_Photovoltaics_until_2014.pdf.

[2] Hoffmann W. A vision for PV technology up to 2030 and beyond—an industry view. Brussels: European Photovoltaic Industry Association; 2004.
[3] Solar photovotaics. A technologist's view. http://www.carboninsights.org/?p=818.
[4] Chiba Y, Islam A, Watanabe Y, Komiya R, Koide N, Han L. Dye-sensitized solar cells with conversion efficiency of 11.1%. Jpn J Appl Phys, Part 2 2006;45(24–28):L638–40.
[5] McConnell RD. Assessment of the dye-sensitized solar cell. Renewable Sust Energy Rev 2002;6(September (3)):271–93.
[6] http://3gsolar.com/tech.html.
[7] http://www.ecn.nl/docs/library/report/2002/rx02042.pdf.
[8] Aitola K, Kaskela A, Halme J, Ruiz V, Nasibulin AG, Kauppinen EI, et al. Single-walled carbon nanotube thin-film counter electrodes for indium tin oxide-free plastic dye solar cells. J Electrochem Soc 2010;157(12):B1831–7.
[9] http://www.asx.com.au/asxpdf/20080527/pdf/319b6m8lzhpv3g.pdf.
[10] http://www.sony.net/Products/SC-HP/cx_news/vol56/pdf/sideview56.pdf.
[11] http://www.g24i.com/pages,indoor-applications,65.html.
[12] Krebs FC, Tromholt T, Jorgensen M. Upscaling of polymer solar cell fabrication using full roll-to-roll processing. Nanoscale 2010;2(6):873–86.
[13] Tanabe N.Recent progress in DSC module panel development at Fujikura Ltd. DSC-IC 2010. 2010.
[14] Kroon JM, Bakker NJ, Smit HJP, Liska P, Thampi KR, Wang P, et al. Nanocrystalline dye-sensitized solar cells having maximum performance. Prog Photovolt 2007;15(1):1–18.
[15] Kalowekamo J, Baker E. Estimating the manufacturing cost of purely organic solar cells. Solar Energy 2009;83(August (8)):1224–31.
[16] Zweibel K. Thin film PV manufacturing: materials costs and their optimization. Sol Energy Mater Sol Cells 2000;63(August (4)):375–86.
[17] Wang Y, Yang H, Liu Y, Wang H, Shen H, Yan J, et al. The use of Ti meshes with self-organized TiO_2 nanotubes as photoanodes of all-Ti dye-sensitized solar cells. Prog Photovolt 2010;18(4):285–90.
[18] http://www.alibaba.com/product-gs/260984640/titanium_foil.html.
[19] http://www.alibaba.com/product-gs/309148412/Household_aluminum_foil.html.
[20] Zweibel K. Issues in thin film PV manufacturing cost reduction. Sol Energy Mater Sol Cells 1999;59(September (1–2)):1–18.
[21] Murakami TN, Graetzel M. Counter electrodes for DSC: application of functional materials as catalysts. Inorg Chim Acta 2008;361(3):572–80.
[22] Ikegami M, Suzuki J, Teshima K, Kawaraya M, Miyasaka T. Improvement in durability of flexible plastic dye-sensitized solar cell modules. Sol Energy Mater Sol Cells 2009;93(6–7):836–9.
[23] Onoda K, Ngamsinlapasathian S, Fujieda T, Yoshikawa S. The superiority of Ti plate as the substrate of dye-sensitized solar cells. Sol Energy Mater Sol Cells 2007;91(August (13)):1176–81.
[24] Ma T, Fang X, Akiyama M, Inoue K, Noma H, Abe E. Properties of several types of novel counter electrodes for dye-sensitized solar cells. J Electroanal Chem 2004;574(1):77–83.
[25] Fang X, Ma T, Akiyama M, Guan G, Tsunematsu S, Abe E. Flexible counter electrodes based on metal sheet and polymer film for dye-sensitized solar cells. Thin Solid Films 2005;472(1–2):242–5.
[26] Toivola M, Ahlskog F, Lund P. Industrial sheet metals for nanocrystalline dye-sensitized solar cell structures. Sol Energy Mater Sol Cells 2006;90(17):2881–93.
[27] Miettunen K, Halme J, Toivola M, Lund P. Initial performance of dye solar cells on stainless steel substrates. J Phys Chem C 2008;112(10):4011–7.
[28] Ngamsinlapasathian S, Onoda K, Takayasu T, Sagawa T, Yoshikawa S. Meeting Abstracts 2010;1001:473.
[29] Wang H, Liu Y, Xu H, Dong X, Shen H, Wang Y, et al. An investigation on the novel structure of dye-sensitized solar cell with integrated photoanode. Renewable Energy 2009;34(June (6)):1635–8.
[30] Kang MG, Park N, Ryu KS, Chang SH, Kim K. A 4.2% efficient flexible dye-sensitized TiO_2 solar cells using stainless steel substrate. Sol Energy Mater Sol Cells 2006;903(March (5)):574–81.
[31] Kang MG, Park N, Ryu KS, Chang SH, Kim K. Flexible metallic substrates for TiO_2 film of dye-sensitized solar cells. Chem Lett 2005;34(6):804–5.
[32] Miettunen K, Halme J, Saukkonen T, Toivola M, Lund PD.Proceedings of the 24th European photovoltaic solar energy conference. 2009.
[33] Asghar MI, Miettunen K, Halme J, Vahermaa P, Toivola M, Aitola K, et al. Review of stability for advanced dye solar cells. Energy Environ Sci 2010;3(4):418–26.
[34] Miettunen K, Ruan X, Saukkonen T, Halme J, Toivola M, Guangsheng H, et al. Stability of dye solar cells with photoelectrode on metal substrates. J Electrochem Soc 2010;157(6):B814–9.
[35] Li D, Li H, Luo Y, Li K, Meng Q, Armand M, et al. Non-corrosive, non-absorbing organic redox couple for dye-sensitized solar cells. Adv Funct Mater 2010;20(19):3358–65.
[36] Pasquier AD, Stewart M, Spitler T, Coleman M. Aqueous coating of efficient flexible TiO_2 dye solar cell photoanodes. Sol Energy Mater Sol Cells 2009;93(April (4)):528–35.
[37] Toivola M, Halme J, Miettunen K, Aitola K, Lund PD. Nanostructured dye solar cells on flexible substrates – review. Int J Energy Res 2009;33(13):1145–60.
[38] Miettunen K, Halme J, Lund P. Segmented cell design for improved factoring of aging effects in dye solar cells. J Phys Chem C 2009;113(23):10297–302.
[39] Miyasaka T, Kijitori Y. Low-temperature fabrication of dye-sensitized plastic electrodes by electrophoretic preparation of mesoporous TiO_2 layers. J Electrochem Soc 2004;151(11):A1767–73.
[40] Scheirs J, Gardette J. Photo-oxidation and photolysis of poly(ethylene naphthalate). Polym Degrad Stab 1997;56(June (3)):339–50.
[41] Zweifel H, Maier RD, Schiler M. Plastic additives handbook. 6th ed. Ohio: Hanser Pubication; 2009. p. 387.
[42] Ngamsinlapasathian S, Sreethawong T, Suzuki Y, Yoshikawa S. Doubled layered ITO/SnO_2 conducting glass for substrate of dye-sensitized solar cells. Sol Energy Mater Sol Cells 2006;90(14):2129–40.
[43] Gruner G. Carbon nanotube films for transparent and plastic electronics. J Mater Chem 2006;16(35):3533–9.
[44] Lewis BG, Paine DC. Transparent conductive oxides. MRS Bull 2000;25:22.
[45] Guldi DM. Nanometer scale carbon structures for charge-transfer systems and photovoltaic applications. Phys Chem Chem Phys 2007;9(12):1400–20.
[46] Kongkanand A, Martinez Dominguez R, Kamat PV. Single wall carbon nanotube scaffolds for photoelectrochemical solar cells. Capture and transport of photogenerated electrons. Nano Lett 2007;7(3):676–80.
[47] Green AA, Hersam MC. Colored semitransparent conductive coatings consisting of monodisperse metallic single-walled carbon nanotubes. Nano Lett 2008;8(5):1417–22.
[48] Hu L, Hecht DS, Gruener G. Percolation in transparent and conducting carbon nanotube networks. Nano Lett 2004;4(12):2513–7.
[49] Saran N, Parikh K, Suh D, Munoz E, Kolla H, Manohar SK. Fabrication and characterization of thin films of single-walled carbon nanotube bundles on flexible plastic substrates. J Am Chem Soc 2004;126(14):4462–3.
[50] Zhou Y, Hu L, Gruner G. A method of printing carbon nanotube thin films. Appl Phys Lett 2006;88(12):123109/1–3.
[51] Fan X, Wang F, Chu Z, Chen L, Zhang C, Zou D. Conductive mesh based flexible dye-sensitized solar cells. Appl Phys Lett 2007;90(7):073501/1–3.
[52] Wang H, Liu Y, Huang H, Zhong M, Shen H, Wang Y, et al. Low resistance dye-sensitized solar cells based on all-titanium substrates using wires and sheets. Appl Surf Sci 2009;255(22):9020–5.
[53] Huang X, Shen P, Zhao B, Feng X, Jiang S, Chen H, et al. Stainless steel mesh-based flexible quasi-solid dye-sensitized solar cells. Sol Energy Mater Sol Cells 2010;94(June (6)):1005–10.
[54] Miettunen K, Toivola M, Halme J, Armentia J, Vahermaa P, Lund P.Proceedings of the 22nd European photovoltaic solar energy conference. 2007. p. 512–5.
[55] Okada K, Matsui H, Kawashima T, Ezure T, Tanabe N. 100 mm × 100 mm large-sized dye sensitized solar cells. J Photochem Photobiol A 2004;164(June (1–3)):193–8.
[56] Chabrecek P. New fabric based electrodes/substrates for DSC solar cells. In: 24th European photovoltaic solar energy conference and exhibition, 21–25 September. 2009.
[57] Park JH, Jun Y, Yun H, Lee S, Kang MG. Fabrication of an efficient dye-sensitized solar cell with stainless steel substrate. J Electrochem Soc 2008;155(7):F145–9.
[58] Yamaguchi T, Tobe N, Matsumoto D, Nagai T, Arakawa H. Highly efficient plastic-substrate dye-sensitized solar cells with validated conversion efficiency of 7.6%. Sol Energy Mater Sol Cells 2010;94(5):812–6.
[59] Ito S, Ha NC, Rothenberger G, Liska P, Comte P, Zakeeruddin SM, et al. High-efficiency (7.2%) flexible dye-sensitized solar cells with Ti-metal substrate for nanocrystalline-TiO_2 photoanode. Chem Commun (Cambridge, UK) 2006;38:4004–6.
[60] http://www.alibaba.com/productgs/340529113/supply_titanium_sheets_best_price.html.
[61] Lindstrom H, Holmberg A, Magnusson E, Lindquist S, Malmqvist L, Hagfeldt A. A new method for manufacturing nanostructured electrodes on plastic substrates. Nano Lett 2001;1(2):97–100.
[62] Pichot F, Ferrere S, Pitts RJ, Gregg BA. Flexible solid-state photoelectrochromic windows. J Electrochem Soc 1999;146(11):4324–6.
[63] Brabec CJ, Padinger F, Hummelen JC, Janssen RAJ, Sariciftci NS. Realization of large area flexible fullerene-conjugated polymer photocells: a route to plastic solar cells. Synth Met 1999;102(1–3):861–4.
[64] Zhang D, Yoshida T, Minoura H. Low temperature synthesis of porous nanocrystalline TiO_2 thick film for dye-sensitized solar cells by hydrothermal crystallization. Chem Lett 2002;9:874–5.
[65] Duerr M, Schmid A, Obermaier M, Rosselli S, Yasuda A, Nelles G. Low-temperature fabrication of dye-sensitized solar cells by transfer of composite porous layers. Nat Mater 2005;4(8):607–11.
[66] Zhang D, Yoshida T, Minoura H. Low-temperature fabrication of efficient porous titania photoelectrodes by hydrothermal crystallization at the solid/gas interface. Adv Mater (Weinheim, Germany) 2003;15(10): 814–7.
[67] Zhang D, Yoshida T, Furuta K, Minoura H. Hydrothermal preparation of porous nanocrystalline TiO_2 electrodes for flexible solar cells. J Photochem Photobiol A 2004;164(1–3):159–66.
[68] Murakami TN, Kijitori Y, Kawashima N, Miyasaka T. UV light-assisted chemical vapor deposition of TiO_2 for efficiency development at dye-sensitized mesoporous layers on plastic film electrodes. Chem Lett 2003;32(11): 1076–7.
[69] Miyasaka T, Kijitori Y, Murakami TN, Kimura M, Uegusa S. Efficient nonsintering type dye-sensitized photocells based on electrophoretically deposited TiO_2 layers. Chem Lett 2002;12:1250–1.
[70] Mincuzzi G, Vesce L, Reale A, Di Carlo A, Brown TM. Efficient sintering of nanocrystalline titanium dioxide films for dye solar cells via raster scanning laser. Appl Phys Lett 2009;95(10):103312/1–3.
[71] Kim H, Pique A, Kushto GP, Auyeung RCY, Lee SH, Arnold CB, et al. Dye-sensitized solar cells using laser processing techniques. In: Proc SPIE-Int Soc Opt Eng. 2004 [5339 (Photon Processing in Microelectronics and Photonics III):348–56].

[72] Kim H, Auyeung RCY, Ollinger M, Kushto GP, Kafafi ZH, Pique A. Laser-sintered mesoporous TiO_2 electrodes for dye-sensitized solar cells. Appl Phys A: Mater Sci Process 2006;83(1):73–6.
[73] Pan H, Ko SH, Misra N, Grigoropoulos CP. Laser annealed composite titanium dioxide electrodes for dye-sensitized solar cells on glass and plastics. Appl Phys Lett 2009;94(7):071117/1–3.
[74] Pichot F, Pitts JR, Gregg BA. Low-temperature sintering of TiO_2 colloids: application to flexible dye-sensitized solar cells. Langmuir 2000;16(13): 5626–30.
[75] Kijitori Y, Ikegami M, Miyasaka T. Highly efficient plastic dye-sensitized photoelectrodes prepared by low-temperature binder-free coating of mesoscopic titania pastes. Chem Lett 2007;36(1):190–1.
[76] Miyasaka T, Ikegami M, Kijitori Y. Photovoltaic performance of plastic dye-sensitized electrodes prepared by low-temperature binder-free coating of mesoscopic titania. J Electrochem Soc 2007;154(5):A455–61.
[77] Lindstrom H, Holmberg A, Magnusson E, Malmqvist L, Hagfeldt A. A new method to make dye-sensitized nanocrystalline solar cells at room temperature. J Photochem Photobiol A 2001;145(1–2):107–12.
[78] Santa-Nokki H, Kallioinen J, Kololuoma T, Tuboltsev V, Korppi-Tommola J. Dynamic preparation of TiO_2 films for fabrication of dye-sensitized solar cells. J Photochem Photobiol A 2006;182(2):187–91.
[79] Kay A, Grätzel M. Low cost photovoltaic modules based on dye sensitized nanocrystalline titanium dioxide and carbon powder. Sol Energy Mater Sol Cells 1996;44(October (1)):99–117.
[80] Halme J, Toivola M, Tolvanen A, Lund P. Charge transfer resistance of spray deposited and compressed counter electrodes for dye-sensitized nanoparticle solar cells on plastic substrates. Sol Energy Mater Sol Cells 2006;90(May (7–8)):872–86.
[81] Papageorgiou N, Maier WF, Gratzel M. An iodine/triiodide reduction electrocatalyst for aqueous and organic media. J Electrochem Soc 1997;144(3):876–84.
[82] Hauch A, Georg A. Diffusion in the electrolyte and charge-transfer reaction at the platinum electrode in dye-sensitized solar cells. Electrochim Acta 2001;46(22):3457–66.
[83] Fang X, Ma T, Guan G, Akiyama M, Kida T, Abe E. Effect of the thickness of the Pt film coated on a counter electrode on the performance of a dye-sensitized solar cell. J Electroanal Chem 2004;570(2):257–63.
[84] Jun Y, Kim J, Kang MG. A study of stainless steel-based dye-sensitized solar cells and modules. Sol Energy Mater Sol Cells 2007;91(9):779–84.
[85] Kim S, Nah Y, Noh Y, Jo J, Kim D. Electrodeposited Pt for cost-efficient and flexible dye-sensitized solar cells. Electrochim Acta 2006;51(18): 3814–9.
[86] Nemoto J, Sakata M, Hoshi T, Ueno H, Kaneko M. All-plastic dye-sensitized solar cell using a polysaccharide film containing excess redox electrolyte solution. J Electroanal Chem 2007;599(1):23–30.
[87] Hara K, Wang Z, Cui Y, Furube A, Koumura N. Long-term stability of organic-dye-sensitized solar cells based on an alkyl-functionalized carbazole dye. Energy Environ Sci 2009;2(10):1109–14.
[88] Nazeeruddin MK, De Angelis F, Fantacci S, Selloni A, Viscardi G, Liska P, et al. Combined experimental and DFT-TDDFT computational study of photoelectrochemical cell ruthenium sensitizers. J Am Chem Soc 2005;127(48):16835–47.
[89] Yong-Seok Park ea. Room temperature flexible and transparent ITO/Ag/ITO electrode grown on flexile PES substrate by continuous roll-to-roll sputtering for flexible organic photovoltaics. J Phys D 2009;42(23):235109.
[90] Chen L, Tan W, Zhang J, Zhou X, Zhang X, Lin Y. Fabrication of high performance Pt counter electrodes on conductive plastic substrate for flexible dye-sensitized solar cells. Electrochim Acta 2010;55(11):3721–6.
[91] Toivola M, Peltola T, Miettunen K, Halme J, Lund P. Thin film nano solar cells from device optimization to upscaling. J Nanosci Nanotechnol 2010;10(2):1078–84.
[92] Miettunen K, Asghar I, Ruan X, Halme J, Saukkonen T, Lund P. Stabilization of metal counter electrodes for dye solar cells. J Electroanal Chem 2011;653:93–9.
[93] Murofushi K, Sato R, Kondo K. US patent no. 2002, 7,157:788.
[94] Sugihara H, Hara K, Arakawa H, Islam A, Singh LP. US patent no. 2000; 6,274:806.
[95] Wang G, Lin Y. Novel counter electrodes based on NiP-plated glass and Ti plate substrate for dye-sensitized solar cells. J Mater Sci 2007;42(13):5281–5.
[96] Chen J, Li K, Luo Y, Guo X, Li D, Deng M, et al. A flexible carbon counter electrode for dye-sensitized solar cells. Carbon 2009;47(11):2704–8.
[97] Pettersson H, Gruszecki T, Schnetz C, Streit M, Xu Y, Sun L, et al. Parallel-connected monolithic dye-sensitised solar modules. Prog Photovolt: Res Appl 2010;18(5):340–5.
[98] Smith T. A review of carbon black pigments. Pigm Resin Technol 1983;12(4):14–6.
[99] Wroblowa HS, Saunders A. Flow-through electrodes: II. The $I_3/^-/I^-$ redox couple. J Electroanal Chem 1973;42(April (3)):329–46.
[100] Pettersson H, Gruszecki T. Long-term stability of low-power dye-sensitised solar cells prepared by industrial methods. Sol Energy Mater Sol Cells 2001;70(2):203–12.
[101] Miettunen K, Toivola M, Hashmi G, Salpakari J, Asghar I, Lund P. A carbon gel catalyst layer for the roll-to-roll production of dye solar cells. Carbon 2010;49:528–32.
[102] Skupien K, Putyra P, Walter J, Kozłowski RH, Khelashvili G, Hinsch A, et al. Catalytic materials manufactured by the polyol process for monolithic dye-sensitized solar cells. Prog Photovolt: Res Appl 2009;17(1):67–73.
[103] Huang Z, Liu X, Li K, Li D, Luo Y, Li H, et al. Application of carbon materials as counter electrodes of dye-sensitized solar cells. Electrochem Commun 2007;9(April (4)):596–8.
[104] Pettersson H, Gruszecki T, Bernhard R, Haeggman L, Gorlov M, Boschloo G, et al. The monolithic multicell: a tool for testing material components in dye-sensitized solar cells. Prog Photovolt 2007;15(2):113–21.
[105] Fu Y, Hou M, liang D, Yan X, Fu Y, Shao Z, et al. The electrical resistance of flexible graphite as flowfield plate in proton exchange membrane fuel cells. Carbon 2008;46(January (1)):19–23.
[106] Frysz CA, Chung DDL. Electrochemical behavior of flexible graphite. Carbon 1997;35(6):858–60.
[107] Suzuki K, Yamaguchi M, Kumagai M, Yanagida S. Application of carbon nanotubes to counter electrodes of dye-sensitized solar cells. Chem Lett 2003;32(1):28–9.
[108] Krishnankutty N, Park C, Rodriguez NM, Baker RTK. The effect of copper on the structural characteristics of carbon filaments produced from iron catalyzed decomposition of ethylene. Catal Today 1997;37(August (3)):295–307.
[109] Iijima S, Yudasaka M, Yamada R, Bandow S, Suenaga K, Kokai F, et al. Nano-aggregates of single-walled graphitic carbon nano-horns. Chem Phys Lett 1999;309(August (3–4)):165–70.
[110] Calogero G, Bonaccorso F, Marago OM, Gucciardi PG, Di MG. Single wall carbon nanotubes deposited on stainless steel sheet substrates as novel counter electrodes for ruthenium polypyridine based dye sensitized solar cells. Dalton Trans 2010;39(11):2903–9.
[111] Aitola K, Halme J, Halonen N, Kaskela A, Toivola M, Nasibulin AG, et al. Design of dye solar cell counter electrodes based on different carbon nanostructures. Thin Solid Films, article in press.
[112] Li Q, Wu J, Tang Q, Lan Z, Li P, Lin J, et al. Application of microporous polyaniline counter electrode for dye-sensitized solar cells. Electrochem Commun 2008;10(September (9)):1299–302.
[113] Wu J, Li Q, Fan L, Lan Z, Li P, Lin J, et al. High-performance polypyrrole nanoparticles counter electrode for dye-sensitized solar cells. J Power Sources 2008;181(June (1)):172–6.
[114] Pringle JM, Armel V, Forsyth M, MacFarlane DR. PEDOT-coated counter electrodes for dye-sensitized solar cells. Aust J Chem 2009;62(4):348–52.
[115] Muto T, Ikegami M, Kobayashi K, Miyasaka T. Conductive polymer-based mesoscopic counter electrodes for plastic dye-sensitized solar cells. Chem Lett 2007;36(6):804–5.
[116] Ahmad S, Yum J, Xianxi Z, Graetzel M, Butt H, Nazeeruddin MK. Dye-sensitized solar cells based on poly(3,4-ethylenedioxythiophene) counter electrode derived from ionic liquids. J Mater Chem 2010;20(9):1654–8.
[117] Ahmad S, Deepa M, Singh S. Electrochemical synthesis and surface characterization of poly(3,4-ethylenedioxythiophene) films grown in an ionic liquid. Langmuir 2007;23(23):11430–3.
[118] Biancardo M, West K, Krebs FC. Quasi-solid-state dye-sensitized solar cells: Pt and PEDOT:PSS counter electrodes applied to gel electrolyte assemblies. J Photochem Photobiol A 2007;187(April (2–3)):395–401.
[119] Saito Y, Kitamura T, Wada Y, Yanagida S. Application of poly(3,4-ethylenedioxythiophene) to counter electrode in dye-sensitized solar cells. Chem Lett 2002;10:1060–1.
[120] Murakami TN, Ito S, Wang Q, Nazeeruddin MK, Bessho T, Cesar I, et al. Highly efficient dye-sensitized solar cells based on carbon black counter electrodes. J Electrochem Soc 2006;153(12):A2255–61.
[121] Ikeda N, Miyasaka T. Plastic and solid-state dye-sensitized solar cells incorporating single-wall carbon nanotubes. Chem Lett 2007;36(3):466–7.
[122] Spath M, Sommeling PM, van Roosmalen JAM, Smit HJP, van der Burg NPG, Mahieu DR, et al. Reproducible manufacturing of dye-sensitized solar cells on a semi-automated baseline. Prog Photovolt 2003;11(3):207–20.
[123] Sastrawan R, Beier J, Belledin U, Hemming S, Hinsch A, Kern R, et al. A glass frit-sealed dye solar cell module with integrated series connections. Sol Energy Mater Sol Cells 2006;90(July (11)):1680–91.
[124] Sastrawan R, Beier J, Belledin U, Hemming S, Hinsch A, Kern R, et al. New interdigital design for large area dye solar modules using a lead-free glass frit sealing. Prog Photovolt: Res Appl 2006;14(8):697–709.
[125] Miettunen K, Halme J, Lund P. Spatial distribution and decrease of dye solar cell performance induced by electrolyte filling. Electrochem Commun 2009;11(January (1)):25–7.
[126] Hagen A, Barkschat A, Dohrmann JK, Tributsch H. Imaging UV photoactivity and photocatalysis of TiO_2-films. Sol Energy Mater Sol Cells 2003;77(April (1)):1–13.
[127] Noda K. Recent developments of high performance dye-sensitized solar cell. In: 3rd International conference on the industrialization of DSC. 2009.
[128] Meng QB, Takahashi K, Zhang XT, Sutanto I, Rao TN, Sato O, et al. Fabrication of an efficient solid-state dye-sensitized solar cell. Langmuir 2003;19(9):3572–4.
[129] Wang P, Dai Q, Zakeeruddin SM, Forsyth M, MacFarlane DR, Graetzel M. Ambient temperature plastic crystal electrolyte for efficient, all-solid-state dye-sensitized solar cell. J Am Chem Soc 2004;126(42):13590–1.
[130] Desilvestro J, Bertoz M, Tulloch S, Tulloch G. Packaging, scaling and commercialization of dye solar cells. In: Presentation at E-MRS 2009 spring meeting. 2009.

[131] Wang M, Chamberland N, Breau L, Moser J, Humphry-Baker R, Marsan B, et al. An organic redox electrolyte to rival triiodide/iodide in dye-sensitized solar cells. Nat Chem 2010;2(5):385–9.
[132] Macht B, Turrión M, Barkschat A, Salvador P, Ellmer K, Tributsch H. Patterns of efficiency and degradation in dye sensitization solar cells measured with imaging techniques. Sol Energy Mater Sol Cells 2002;73(June (2)):163–73.
[133] Sirimanne PM, Jeranko T, Bogdanoff P, Fiechter S, Tributsch H. On the photodegradation of dye sensitized solid-state TiO_2|dye|CuI cells 2003;18:708–12.
[134] Kawano R, Matsui H, Matsuyama C, Sato A, Susan MABH, Tanabe N, et al. High performance dye-sensitized solar cells using ionic liquids as their electrolytes. J Photochem Photobiol A 2004;164(June (1–3)):87–92.
[135] Papageorgiou N, Athanassov Y, Armand M, Bonhote P, Pettersson H, Azam A, et al. The performance and stability of ambient temperature molten salts for solar cell applications. J Electrochem Soc 1996;143(10):3099–108.
[136] Wang P, Zakeeruddin SM, Moser J, Graetzel M. A new ionic liquid electrolyte enhances the conversion efficiency of dye-sensitized solar cells. J Phys Chem B 2003;107(48):13280–5.
[137] Ito S, Zakeeruddin SM, Humphry-Baker R, Liska P, Charvet R, Comte P, et al. High-efficiency organic-dye-sensitized solar cells controlled by nanocrystalline-TiO_2 electrode thickness. Adv Mater (Weinheim, Germany) 2006;18(9):1202–5.
[138] Pettersson H, Gruszecki T, Johansson L, Johander P. Manufacturing method for monolithic dye-sensitised solar cells permitting long-term stable low-power modules. Sol Energy Mater Sol Cells 2003;77(June (4)):405–13.
[139] Abraham KM. In: Scrosati B, editor. Application of electroactive polymer. London: Chapman & Hall; 1993.
[140] Wang P, Zakeeruddin SM, Exnar I, Graetzel M. High efficiency dye-sensitized nanocrystalline solar cells based on ionic liquid polymer gel electrolyte. Chem Commun (Cambridge, UK) 2002;24:2972–3.
[141] Kubo W, Kitamura T, Hanabusa K, Wada Y, Yanagida S. Quasi-solid-state dye-sensitized solar cells using room temperature molten salts and a low molecular weight gelator. Chem Commun 2002:374–5.
[142] Kato T, Fujimoto M, Kado T, Sakaguchi S, Kosugi D, Shiratuchi R, et al. Additives for increased photoenergy conversion efficiencies of quasi-solid, dye-sensitized solar cells. J Electrochem Soc 2005;152(6):A1105–8.
[143] Ileperuma OA, Kumara GRA, Murakami K. Quasi-solid polymer electrolytes based on polyacrylonitrile and plasticizers for indoline dye sensitized solar cells of efficiency 5.3%. Chem Lett 2008;37(1):36–7.
[144] Yang Y, Zhou CH, Xu S, Zhang J, Wu SJ, Hu H, et al. Optimization of a quasi-solid-state dye-sensitized solar cell employing a nanocrystal–polymer composite electrolyte modified with water and ethanol. Nanotechnology 2009;20(10):105204.
[145] Lee Y, Shen Y, Yang Y. A hybrid PVDF-HFP/nanoparticle gel electrolyte for dye-sensitized solar cell applications. Nanotechnology 2008;19(45):455201/1–6.
[146] Wang P, Zakeeruddin SM, Grätzel M. Solidifying liquid electrolytes with fluorine polymer and silica nanoparticles for quasi-solid dye-sensitized solar cells. J Fluorine Chem 2004;125(August (8)):1241–5.
[147] Priya ARS, Subramania A, Jung Y, Kim K. High-performance quasi-solid-state dye-sensitized solar cell based on an electrospun PVdF-HFP membrane electrolyte. Langmuir 2008;24(17):9816–9.
[148] Premalal EVA, Kumara GRRA, Rajapakse RMG, Shimomura M, Murakami K, Konno A. Tuning chemistry of CuSCN to enhance the performance of TiO_2/N719/CuSCN all-solid-state dye-sensitized solar cell. Chem Commun (Cambridge, UK) 2010;46(19):3360–2.
[149] Ding I, Melas-Kyriazi J, Cevey-Ha N, Chittibabu KG, Zakeeruddin SM, Grätzel M, et al. Deposition of hole-transport materials in solid-state dye-sensitized solar cells by doctor-blading. Org Electron 2010;11(July (7)):1217–22.
[150] Tétreault N, Horváth E, Moehl T, Brillet J, Smajda R, Bungener S, et al. High efficiency solid state dye sensitized solar cells: fast charge extraction through self-assembled 3D fibrous network of crystalline TiO_2 nanowires. ACS Nano 2010;4(12):7644–50.
[151] Stergiopoulos T, Arabatzis IM, Katsaros G, Falaras P. Binary polyethylene oxide/titania solid-state redox electrolyte for highly efficient nanocrystalline TiO_2 photoelectrochemical cells. Nano Lett 2002;2(11):1259–61.
[152] Nei de Freitas J, Longo C, Nogueira AF, De Paoli M. Solar module using dye-sensitized solar cells with a polymer electrolyte. Sol Energy Mater Sol Cells 2008;92(September (9)):1110–4.
[153] Han H, Bach U, Cheng Y, Caruso RA. Increased nanopore filling: effect on monolithic all-solid-state dye-sensitized solar cells. Appl Phys Lett 2007;90(21):213510/1–3.
[154] Han H, Bach U, Cheng Y, Caruso RA, MacRae C. A design for monolithic all-solid-state dye-sensitized solar cells with a platinized carbon counter electrode. Appl Phys Lett 2009;94(10):103102/1–3.
[155] Thompson SJ, Duffy NW, Bach U, Cheng Y. On the role of the spacer layer in monolithic dye-sensitized solar cells. J Phys Chem C 2010;114(5):2365–9.
[156] Tennakone K, Kumara GRRA, Kottegoda IRM, Wijayantha KGU, Perera VPS. A solid-state photovoltaic cell sensitized with a ruthenium bipyridyl complex. J Phys D: Appl Phys 1998;31(12):1492–6.
[157] Kumara GRRA, Konno A, Senadeera GKR, Jayaweera PVV, De Silva DBRA, Tennakone K. Dye-sensitized solar cell with the hole collector p-CuSCN deposited from a solution in n-propyl sulphide. Sol Energy Mater Sol Cells 2001;69(September (2)):195–9.
[158] Rost C, Sieber I, Fischer C, Lux-Steiner MC, Könenkamp R. Semiconductor growth on porous substrates. Mater Sci Eng B 2000;69–70(January):570–3.
[159] Smestad GP, Spiekermann S, Kowalik J, Grant CD, Schwartzberg AM, Zhang J, et al. A technique to compare polythiophene solid-state dye sensitized TiO_2 solar cells to liquid junction devices. Sol Energy Mater Sol Cells 2003;76(February (1)):85–105.
[160] Kumara GRA, Kaneko S, Okuya M, Tennakone K. Fabrication of dye-sensitized solar cells using triethylamine hydrothiocyanate as a CuI crystal growth inhibitor. Langmuir 2002;18(26):10493–5.
[161] Zhang X, Taguchi T, Wang H, Meng Q, Sato O, Fujishima A. Investigation of the stability of solid-state dye-sensitized solar cells. Res Chem Intermed 2007;33(1–2):5–11.
[162] Kumara GRA, Konno A, Shiratsuchi K, Tsukahara J, Tennakone K. Dye-sensitized solid-state solar cells: use of crystal growth inhibitors for deposition of the hole collector. Chem Mater 2002;14(3):954–5.
[163] Yum J, Chen P, Gratzel M, Nazeruddin MK. Recent developments in solid-state dye-sensitized solar cells. ChemSusChem 2008;1(8–9):699–707.
[164] Schmidt-Mende L, Grätzel M. TiO_2 pore-filling and its effect on the efficiency of solid-state dye-sensitized solar cells. Thin Solid Films 2006;500(1–2):296–301.
[165] Snaith HJ, Schmidt-Mende L. Advances in liquid-electrolyte and solid-state dye-sensitized solar cells. Adv Mater (Weinheim, Germany) 2007;19(20):3187–200.
[166] Fabregat-Santiago F, Bisquert J, Cevey L, Chen P, Wang M, Zakeeruddin SM, et al. Electron transport and recombination in solid-state dye solar cell with Spiro-OMeTAD as hole conductor. J Am Chem Soc 2009;131(2):558–62.
[167] Fabregat-Santiago F, Bisquert J, Palomares E, Haque SA, Durrant JR. Impedance spectroscopy study of dye-sensitized solar cells with undoped spiro-OMeTAD as hole conductor. J Appl Phys 2006;100(3):034510/1–7.
[168] Ding I, Tétreault N, Brillet J, Hardin BE, Smith EH, Rosenthal SJ, et al. Pore-filling of Spiro-OMeTAD in solid-state dye sensitized solar cells: quantification, mechanism, and consequences for device performance. Adv Funct Mater 2009;19(15):2431–6.
[169] Snaith HJ, Baker RH, Chen P, Cesar I, Zakeeruddin SM, Grätzel M. Charge collection and pore filling in solid-state dye-sensitized solar cells. Nanotechnology 2008;19:424003 [12].
[170] Saito Y, Fukuri N, Senadeera R, Kitamura T, Wada Y, Yanagida S. Solid state dye sensitized solar cells using in situ polymerized PEDOTs as hole conductor. Electrochem Commun 2004;6(January (1)):71–4.
[171] Chen P, Yum JH, De Angelis F, Mosconi E, Fantacci S, Moon S, et al. High open-circuit voltage solid-state dye-sensitized solar cells with organic dye. Nano Lett 2009;9(6):2487–92.
[172] Wang M, Xu M, Shi D, Li R, Gao F, Zhang G, et al. High-performance liquid and solid dye-sensitized solar cells based on a novel metal-free organic sensitizer. Adv Mater 2008;20(23):4460–3.
[173] Stathatos E, Lianos P, Lavrencic-Stangar U, Orel B. A High-performance solid-state dye-sensitized photoelectrochemical cell employing a nanocomposite gel electrolyte made by the sol–gel route. Adv Mater 2002;14(5):354–7.
[174] Lan Z, Wu J, Lin J, Huang M. Dye-sensitized solar cell with a solid state organic-inorganic composite electrolyte containing catalytic functional polypyrrole nanoparticles. J Sol–Gel Sci Technol 2010;53(3):599–604.
[175] Matsui H, Okada K, Kitamura T, Tanabe N. Thermal stability of dye-sensitized solar cells with current collecting grid. Sol Energy Mater Sol Cells 2009;93(June (6–7)):1110–5.
[176] Hinsch A, Kroon JM, Kern R, Uhlendorf I, Holzbock J, Meyer A, et al. Long-term stability of dye-sensitised solar cells. Prog Photovolt: Res Appl 2001;9(6):425–38.
[177] http://www.tapecase.com/p.487.108/3m-adhesive-transfer-tape-2-mil-3m467mpf.aspx.
[178] Lilliedal MR, Medford AJ, Madsen MV, Norrman K, Krebs FC. The effect of post-processing treatments on inflection points in current–voltage curves of roll-to-roll processed polymer photovoltaics. Sol Energy Mater Sol Cells 2010;94(December (12)):2018–31.
[179] http://www.swisslaser.net/libraries.files/Vortrag_kiy.pdf.
[180] http://www2.dupont.com/Photovoltaics/en_US/products_services/frontsheet/teonexPEN_melinexST.html.
[181] http://www2.dupont.com/Surlyn/en_US/assets/downloads/surlyn_1601_2lm.pdf.
[182] Ramasamy E, Lee WJ, Lee DY, Song JS. Portable, parallel grid dye-sensitized solar cell module prepared by screen printing. J Power Sources 2007;165(February (1)):446–9.
[183] Yeon DH, Kim KK, Park NG, Cho YS. Bismuth borosilicate-based thick film passivation of Ag grid for large-area dye-sensitized solar cells. J Am Ceram Soc 2010;93(6):1554–6.
[184] Grätzel M. Perspectives for dye-sensitized nanocrystalline solar cells. Prog Photovolt: Res Appl 2000;8(1):171–85.
[185] Kurth M. US Patent US6462266B1; 2002.
[186] Goldstein JR. US Patent US2005072458 (A1); 2005.
[187] Dai S, Weng J, Sui Y, Chen S, Xiao S, Huang Y, et al. The design and outdoor application of dye-sensitized solar cells. Inorg Chim Acta 2008;361(February (3)):786–91.
[188] Han L, Fukui A, Fuke N, Koide N, Yamanaka R.Conference record of the IEEE 4th world conference on photovoltaic energy conversion. 2006.
[189] Seo H, Son M, Hong J, Lee D, An T, Kim H, et al. The fabrication of efficiency-improved W-series interconnect type of module by balancing the performance of single cells. Sol Energy 2009;83(December (12)):2217–22.

[190] Han L, Fukui A, Chiba Y, Islam A, Komiya R, Fuke N, et al. Integrated dye-sensitized solar cell module with conversion efficiency of 8.2%. Appl Phys Lett 2009;94(1):013305/1–3.
[191] Tulloch GE. Light and energy dye solar cells for the 21st century. J Photochem Photobiol A 2004;164(June (1–3)):209–19.
[192] Fukui A, Fuke N, Komiya R, Koide N, Yamanaka R, Katayama H, et al. Dye-sensitized photovoltaic module with conversion efficiency of 8.4%. Appl Phys Express 2009;2(8):082202/1–3.
[193] Sastrawan R, Renza J, Prahl C, Beier J, Hinsch A, Kerna R. Interconnecting dye solar cells in modules—*I*–*V* characteristics under reverse bias. J Photochem Photobiol A 2006;178:33–40.
[194] Hinsch A, Belledin U, Brandt H, Einsele F, Hemming S, Koch D, et al. Glass frit sealed dye solar modules with adaptable screen printed design. In: Proceedings of the IEEE fourth world conference on photovoltaic energy conversion. 2006.
[195] Hinsch A, Behrens S, Berginc M, Bönnemann H, Brandt H, Drewitz A, et al. Material development for dye solar modules: results from an integrated approach. Prog Photovolt: Res Appl 2008;16(6):489–501.
[196] Kato N, Takeda Y, Higuchi K, Takeichi A, Sudo E, Tanaka H, et al. Degradation analysis of dye-sensitized solar cell module after long-term stability test under outdoor working condition. Sol Energy Mater Sol Cells 2009;93(June (6–7)):893–7.
[197] http://www.3gsolar.com/NewsItem.aspx?ID=26.
[198] Krebs FC, Spanggard H, Kjær T, Biancardo M, Alstrup J. Large area plastic solar cell modules. Mater Sci Eng B 2007;138(March (2)):106–11.